Thesis Title

Inauguraldissertation

der Philosophisch-naturwissenschaftlichen Fakultät

der Universität Bern

vorgelegt von

RAPHAEL WOLFISBERG

von Neuenkirch, LU

Leiter der Arbeit

Prof. Dr. Christoph Kempf

and

Dr. Carlos Ros

Departement für Chemie und Biochemie

E r k l ä r u n g

gemäss Art. 28 Abs. 2 RSL 05

Name/Vorname: ....

Matrikelnummer: ....

Studiengang: ……………………………………………………………………

Bachelor ☐　　　Master ☐　　　Dissertation ☐

Titel der Arbeit: ....

....

....

LeiterIn der Arbeit: ....

....

Ich erkläre hiermit, dass ich diese Arbeit selbständig verfasst und keine anderen als die angegebenen Quellen benutzt habe. Alle Stellen, die wörtlich oder sinngemäss aus Quellen entnommen wurden, habe ich als solche gekennzeichnet. Mir ist bekannt, dass andernfalls der Senat gemäss Artikel 36 Absatz 1 Buchstabe r des Gesetztes vom 5. September 1996 über die Universität zum Entzug des auf Grund dieser Arbeit verliehenen Titels berechtigt ist.

Ich gewähre hiermit Einsicht in diese Arbeit.

....
Ort/Datum

....
Unterschrift

The Thesis Abstract is written here (and usually kept to just this page). The page is kept centered vertically so can expand into the blank space above the title too...

Nomenclature

AAV	Adeno-associated virus
AMDV	Aleutian mink disease virus
B19V	Human parvovirus B19
Bp	Base pair
BPV	Bovine parvovirus
ChPV	Chicken parvovirus
CPV	Canine parvovirus
CV	Column volume
Da	Dalton
DMEM	Dulbecco modified Eagle's medium
DNA	Deoxyribonucleic acid
DPV	Duck parvovirus
dsDNA	Double stranded DNA
EPC	Erythroid progenitor cell
FCS	Fetal calf serum
FPV	Feline parvovirus
GFAV	Gray fox amdovirus
GmDNV	Galleria mellonella densovirus
GPV	Goose parvovirus
HBoV	Human Bocavirus
HBV	Hepatitis B virus
HCV	Hepatitis C virus
HIV	Human immunodeficiency virus
IF	Immunofluorescence
IP	Immunoprecipitation
ITR	Inverted terminal repeat
Kb	Kilo base
kDa	Kilodalton
KRV	Kilham rat virus
mAb	Monoclonal antibody
MVM	Minute virus of mice

MVMi	Immunosuppressive strain of MVM
MVMp	Prototype strain of MVM
NIH	National institutes of health
Nt	Nucleotide
ORF	Open reading frame
PARV4	Parvovirus 4
PCR	Polymerase chain reaction
PEC	Poult enteritis complex
PEMS	Poult enteritis mortality syndrome
PLA_2	Phospholipase A2
PPV	Porcine parvovirus
PstDNV	Penaeus stylirostris densovirus
qPCR	Quantitative PCR
RF	Replicative form
RNA	Ribonucleic acid
RSS	Runting-stunting syndrome
SCID	Severe combined immunodeficiency
SN	Supernatant
ssDNA	Single stranded DNA
SV40	Simian vacuolating virus 40 or Simian virus 40
TuPV	Turkey parvovirus
VP1u	VP1 unique region

Contents

II   Publication   23

III   Discussion   37

List of Figures

List of Tables

Part I

Introduction

1 Introduction

1.1 Discovery and brief history

Minute virus of mice (MVM) is a small, non-enveloped autonomous replicating parvovirus. Nowadays, two variant forms of MVM, that share 96 % nucleotide sequence identity [1], have been discovered independently. First, MVMp, the prototype strain, was isolated and characterized by Crawford in 1966. It originated from a contaminated murine adenovirus stock and was shown to replicate efficiently in mouse fibroblasts [2]. The virus was plaque purified in 1972 [3] and the resulting strain was designated MVM(p) for prototype [4]. Secondly, another strain was recovered from the culture fluid of infected murine EL-4 T-cell lymphoma cells by Bonnard and colleagues in 1976 [5]. This strain efficiently replicates in lymphocytes and is immunosuppressive for allogeneic mixed leukocyte cultures as it inhibits the generation of cytolytic T lymphocytes [6]. Therefore, it was referred to as immunosuppressive strain MVMi [7]. Both strains are well characterized and reciprocally restricted for growth in each other's murine host cell.

Since its discovery nearly 50 years ago, MVM served as an interesting model virus to dissect the molecular mechanisms of tissue tropism, capsid dynamics associated with endosomal trafficking, as well as viral DNA replication and packaging. Furthermore, it gained increasing interest as an important tool for cancer therapy due to its oncolytic capabilities and currently represents a commonly accepted parvovirus model.

1.2 Morphology

Parvoviruses belong to the smallest of isometric viruses. A linear single-stranded DNA genome of about 5 kb is packaged into the virus capsid [8, 9, 10]. They are non-enveloped and their diameters range from 215 Å (Penaeus stylirostris densovirus, PstDNV) to 255 Å (CPV). The icosahedral nature of parvoviruses was shown unambiguously by X-ray crystallography. The capsid surface of some, particularly invertebrate, parvoviruses appears to be smooth (Galleria mellonella densovirus, GmDNV) whereas others (Adeno-associated virus-2, AAV-2) are spiky at the 3- or 5-fold symmetry axes [11, 12].

1.3 Physicochemical properties

Infectious parvovirus virions are composed of about 75 % protein and 25 % DNA. Their molecular weight is approximately 5.5-6.2 x 10^6 Da. The virion buoyant density is 1.39 to 1.43 gcm^{-3}, measured in CsCl gradients [13, 14]. Since parvoviruses are devoid of a lipid envelope, mature virions are stable in the presence of lipid solvents. In particular, animal parvoviruses show considerable heat resistance. Most species remain stable and infectious on exposure to pH 7-9 or incubation at 56 ℃ for 60 min [15, 16, 17, 18]. Only harsh conditions, such as treatment with formalin, β-propiolacetone, hydroxylamine, ultraviolet light, and oxidizing agents as for example sodium hypochlorite ensure effective virus inactivation [19, 20, 21, 22].

1.4 Taxonomy

The classification of the *Parvoviridae* family is based on morphological and functional characteristics. Parvoviruses are ubiquitous pathogens that belong to the smallest DNA-containing viruses. Hence, the prefix "parvum" that means small in Latin. The name "parvovirus" was first introduced to the literature by Carlos Brailovsky, in an early attempt to establish a latinized binomial taxonomy system for viruses, in 1966 [23]. The age of the *Parvoviridae* family may exceed 40 to 50 million years [24]. Apart from their ancient history, the genomes of parvoviruses were affirmed to display similar high mutation rates to RNA viruses [25, 26, 27, 28, 29, 30]. Such high mutation rates in conjunction with the long history might be a reason for the vast genetic divergence and extensive diversity seen within the *Parvoviridae* family. The *Parvoviridae* family comprises of non-enveloped, isometric viruses that contain linear single-stranded DNA genomes. Indeed, parvoviruses are the only viruses in the known biosphere that have both single-stranded and linear DNA genomes. The encapsidated single genomic molecule is 4-6 kb in length and terminates in palindromic duplex hairpin telomers. In general, there are two large open reading frames, ORF1 and ORF2, encoding for the non-structural protein(s) and the capsid protein(s), respectively. In some cases, an additional ORF3 has been identified that encodes an accessory protein, such as NP1, a non-structural protein only found in members of the genus *Bocaparvovirus* and in PPV4 a member of the genus *Copiparvovirus* [31, 32, 33]. As a consequence of such a simple genome, parvoviruses are highly dependent on their host for diverse functions in their reproduction [34, 11]. The terminal hairpins are fundamental for the unique replication strategy of the *Parvoviridae* family and serve as an invariant hallmark for classification. Members of the family *Parvoviridae* infect a wide variety of hosts, ranging from insects to primates. Depending on their host range, the *Parvoviridae* are subdivided into *Parvovirinae* infecting vertebrates

and *Densovirinae* infecting insects and other arthropods, respectively. The *Parvovirinae* subfamily is further subdivided into eight genera: *Amdoparvovirus*, *Aveparvovirus*, *Bocaparvovirus*, *Copiparvovirus*, *Dependoparvovirus*, *Erythroparvovirus*, *Protoparvovirus*, and *Tetraparvovirus* [35]. The subdivision into the eight genera is based on differences in transcription maps, organization of the ITRs, the ability to replicate efficiently either autonomously or with helper virus, the sense of the ssDNA that is packaged into separate virions, and sequence homology amongst the *Parvovirinae* subfamily [36, 12].

1.4.1 The *Parvovirinae* subfamily

Amdoparvovirus

Mature virions exclusively contain negative strand genomic DNA of approximately 4.8 kb in length harbouring dissimilar palindromic sequences at each end [37, 38]. A single promoter located at map unit 3 at the left end of the genome generates all mRNA transcripts of AMDV. Polyadenylation may occur at either the proximal site or at the distal site of the genome. Thus, the transcription profile of the genus *Amdoparvovirus* most closely resembles that of the genus *Erythroparvovirus* [39]. Only two distant species have been reported. Firstly, *Carnivore amdoparvovirus 1*, which comprises only Aleutian mink disease virus (AMDV) and secondly, *Carnivore amdoparvovirus 2*, which encompasses solely gray fox amdovirus (GFAV) [40]. Permissive replication is tightly restricted to Crandell feline kidney cells. The virion surface displays three mounds elevated around the threefold icosahedral axis of symmetry. Several structure features were ascertained to be similar to those found in B19V, CPV, FPV, and MVM. Such appearance is comparable to those observed for the genus *Dependoparvovirus* [41]. Remarkably, there is no evidence of a phospholipase 2A enzymatic core within the naturally truncated N-VP1 terminus of members belonging to the genus *Amdoparvovirus* as it is common to the other genera of the subfamily *Parvovirinae* [12].

Aveparvovirus

Aveparvovirus is a new genus within the *Parvovirinae* subfamily that comprises of the species chicken parvovirus and turkey parvovirus. The name *Aveparvovirus* is derived from <u>av</u>ian parvoviruses, referring to the hosts from which the members were isolated. Although these viruses were identified for years in the intestinal tracts of poultry [42, 43, 44], analysis of the complete nucleotide sequence has been reported only recently. Phylogenetic study of the genomic sequences revealed that interestingly, ChPV and TuPV do not group phylogenetically with GPV and DPV, that are members of the genus *Dependoparvovirus*. It was clearly demonstrated that ChPV, along with the

closely related TuPV, represents the prototype of a novel genus within the *Parvoviri-nae* subfamily [45, 46]. Identical direct repeat sequences flank the genome at both the 3' and the 5' end. Each of which contains a 39 nt ITR that is predicted to form a hairpin structure. ChPV and TuPV feature an overall genome organization similar to that of members of the genus *Bocaparvovirus* [47]. Although it has been demonstrated that ChPV can induce clinical signs in broiler chickens that show characteristics of the runting-stunting syndrome (RSS) [48], the role of avian parvoviruses in the aetiology of enteric diseases in poultry still remains to be demonstrated. RSS, also referred to as mal-absorption syndrome, is characterized by significantly decreased egg hatchability, poorly developed hatched chickens, serious growth retardation, diarrhoea, enteritis, disturbed feathering, low vitality, and bone disorders [49, 50, 51]. Currently, the pathogenicity of TuPV has not been investigated yet. The predominant enteric diseases in turkeys are known as poult enteritis complex (PEC) [52] or the more drastic poult enteritis mortality syndrome (PEMS) [53]. Understanding the role of avian parvoviruses in PEMS, PEC, and RSS is of great interest due to the economic losses resulting from enteric diseases in poultry. [46].

Bocaparvovirus

The name of the genus is derived from <u>bo</u>vine and <u>ca</u>nine, referring to the two hosts of the first identified members of this genus. The genomes of members of the genus *Bocaparvovirus* are quite distinct from all other viruses in the subfamily *Parvovirinae*. As the members of the genera *Protoparvovirus* and *Amdoparvovirus* they contain non-identical imperfect palindromic sequences at both ends of their 5.5 kb genome. Mature virions contain mainly, but not exclusively, negative strand ssDNA [54, 55]. All RNA transcripts are generated from a single P4 promoter at the left-hand end of the genome. The transcripts are alternatively spliced and polyadenylated either at an internal site or at the 3'-end of the genome [56]. Noteworthy, bovine parvovirus (BPV), the main representative, encodes a 22.5 kDa nuclear phosphoprotein, NP1, whose function still remains unknown. This protein is distinct from any other parvovirus-encoded polypeptide [31]. A human bocavirus was first described in 2005, when it was detected in nasopharyn-geal aspirates of young children with respiratory tract infection [57, 58]. More recently, HBoV has been identified in diarrheal feces of children with gastroenteritis [59]. HBoV infection is associated with acute respiratory symptoms and is usually detected in chil-dren under 2 years of age [60, 61, 62]. HBoV infections have been reported world-wide and HBoV was often isolated in respiratory samples of diseased as well as asymptomatic patients sometimes long after the primary infection. Therefore, it can be frequently detected even though it is not likely acting as a pathogen, thus complicating the use of

PCR in diagnostics. Furthermore, long-term persistence may explain that HBoV infection among adults was predominantly reported in association with immunosuppression or immunodeficiency [62, 63].

Copiparvovirus

Based on phylogenetic analysis, the genus *Copiparvovirus* encompasses PPV4 and BPV2. PPV4 was identified in clinical samples from swine herds [33, 64, 65] and represents a distinct branch together with BPV2 [57]. The name *Copiparvovirus* refers to <u>co</u>ws and <u>pi</u>gs, the hosts from which members of that genus were isolated. PPV4 is unique in that it is phylogenetically most closely related to BPV2 but the coding capacity and genome organization resemble more those of viruses of the genus *Bocaparvovirus*. While the ORF3 encoded proteins of the three recognized *Bocaparvovirus* members share amino acid identities of 43.3-47.0 % among themselves, the PPV4 ORF3 encoded protein does not display homology with any protein in the GenBank database [33, 64]. Recently, two novel porcine parvoviruses, PPV5 and PPV6, were discovered [66, 67]. Characterization of their nucleotide sequences revealed that their full-length genomes are approximately 6 kb in length. As a consequence of this capacious genome size, especially their capsid protein encoding genes are exceptionally large. Interestingly, the genomic organization of PPV5 and PPV6 is different from PPV4 in that they lack the extra ORF3 in the middle of the genome. Moreover, PPV5 as well as PPV6 possess the conserved putative secretory PLA_2 motif which is present in the capsid protein of most parvoviruses but is lacking in PPV4. In spite of considerable differences in the genomic organization between BPV2, PPV5, and PPV6 on one hand and PPV4 on the other hand, phylogenetic analysis revealed a close evolutionary relationship of these viruses, suggesting that they share the same immediate ancestor [68, 67]. Since members of the genus *Copiparvovirus* were discovered quite recently, their biological characteristics, relatedness to disease, and potential clinical manifestations are still not fully understood [33, 64, 68, 67]. Especially, Kresse strain of porcine parvovirus belonging to the genus *Protoparvovirus* is known to be an important pathogen responsible for embryonic and fetal death in piglets, resulting in considerable losses in the pig industry worldwide [69, 70, 71, 72]. In order to clarify the precise role of the most recently discovered members of the genus *Copiparvovirus* as causative agents of reproductive failure in breeding animals, more comprehensive epidemiologic studies are required in the future [67].

Dependoparvovirus

Positive and negative strand ssDNA is distributed indifferently among mature virions belonging to the genus *Dependoparvovirus* [73, 9]. The 4.7 kb DNA molecule contains

identical ITRs of 145 nt, the first 125 nt of which form a palindromic sequence [74]. Three mRNA promoters that are located at map units 5, 19, and 40 initiate transcription that can be terminated in two polyadenylation sites located at the right-hand end or alternatively, in the middle of the genome [75, 76]. Common for all currently accepted replication-defective members of the genus *Dependoparvovirus* is their strict dependence upon helper adenoviruses or herpesviruses [77, 78, 79]. Therefore, their host range tropism strongly depends on the one of the helper virus. The only exceptions are the autonomously replicating duck and goose parvoviruses which are also comprised within the *Dependoparvovirus* genus based on phylogenetic analysis [12]. The most important members of this genus are the adeno-associated viruses (AAV). They attracted considerable interests since at least one of them, AAV-2, has been reported to integrate site-specifically into human chromosome 19 [80, 81, 82, 83]. This characteristic makes AAV a promising candidate for creating viral vectors for gene therapy [84, 85]. As a well characterized member of the *Dependoparvoviruses* AAV-2 represents the model virus among this genus.

Erythroparvovirus

Equivalent numbers of positive and negative sense ssDNA are packaged into infectious virions of the genus *Erythroparvovirus*. As in the case with the genus *Dependoparvovirus*, the 5.5 kb ssDNA molecule contains identical ITRs of 383 nt in length at both the 3' and the 5' end. The first 365 nt of those secondary elements form palindromic sequences [86]. Transcription is regulated by a single mRNA promoter located at map unit 6 [87]. A distal polyadenylation site for use in termination of RNA synthesis is located at the far right side. Additionally, transcripts may be terminated at an unusual internal polyadanylation site in the middle of the genome [88]. Viruses belonging to this genus are highly erythrotropic, meaning that efficient replication only occurs in rapidly dividing erythroid progenitor cells (EPCs) such as erythroblasts and megakaryocytes present in the bone marrow. B19V, a widespread human pathogen that causes fifth disease, polyarthropathia, anemic crises in children with underlying hematological diseases (e.g. sickle cell anemia or thalassemia) and intrauterine infections (with hydrops fetalis in some cases) [89] represents the model virus among the genus *Erythroparvovirus*.

Protoparvovirus

Kilham Rat virus (KRV), a member of the genus *Protoparvoviruses* was the first member of the subfamily *Parvovirinae* to be discovered in 1959 [90]. Some members of the genus contain positive strand DNA in variable proportions up to 50 % [91]. However, in mature virions of most members, virtually only negative strand DNA occurs. What

they have in common are their hairpin structures at both the 5' and 3' ends of the linear 5 kb ssDNA molecule that differ in both sequence and predicted structure [92]. Transcription of the genome is regulated by two mRNA promoters at map units 4 and 39 [93]. There is only one polyadenylation site at the 3' end. Viral replication provokes characteristic cytopathic effects in cell culture. Many species display hemagglutination with erythrocytes of one or several species, but not enforcedly of their natural host [94]. The genus *Protoparvovirus* is primarily represented by MVM [12, 95].

Tetraparvovirus

The genus *Tetraparvovirus* is a new genus that arose recently. To date, six species have been discovered, which were isolated from humans [96], chimpanzees, baboons [97], cows, pigs [98, 99, 100], as well as sheep [101]. RNA transcripts that encode the NS-proteins or the VP-proteins are generated from two promoters that are located at map units 6 and 38, respectively. Transcription can be terminated in two polyadenylation sites located at the right-hand end of the genome or alternatively, at an internal polyadenylation site. Since the full-length genome has not been sequenced yet, information of the terminal repeats is still lacking [102]. Analysis of the NS1 protein revealed a G2/M cell cycle arrest induced in NS1-expressing hematopoietic stem cells that clearly involved the predicted helicase motifs [103, 104, 105] of NS1. To date, no PLA$_2$-like activity of expressed VP1u polypeptides has been demonstrated for any member of the genus *Tetraparvovirus* [102]. PARV4 is one of the only four groups of parvoviruses that is known to infect humans besides B19V, HBoV, and AAV. It was first reported in an intravenous drug user who was positive for HBV infection in 2005. The patient suffered from arthralgia, confusion, diarrhea, fatigue, neck stiffness, night sweat, pharyngitis, and vomiting. PARV4 represents a phylogenetic deeply rooted lineage between avian dependoviruses and bovine parvovirus type 3 [96]. So far, most evidence about PARV4 transmission comes from patients who had engaged in high risk behaviour for blood borne viral infections, where PARV4 infection basically was observed to be strongly associated with HCV and HIV infection [106, 107, 108]. However, there are several reports of parenteral transmission in the absence of HIV, HBC, or HCV. PARV4 IgG has been documented independently from other blood borne viruses among injecting drug users [109], in haemophilia patients [110], and in patients who were subjected to intra-muscular injections in the past [111]. Currently, no definitive clinical syndrome was associated with PARV4 infection and there is no evidence for a potential pathogenicity of related members of the genus *Tetraparvovirus* in animals [98]. PARV4 viraemia appears to be asymptomatic [112] and co-existing blood borne viruses do not increase severity [107].

Table 1.1: The type species for each genus is indicated in bold type. [35]

Genus	Species	Virus or virus variants	Abbr.	ACNO[1]
Amdoparvovirus	**Carnivore amdoparvovirus 1**	Aleutian mink disease virus	AMDV	JN040434
	Carnivore amdoparvovirus 2	Gray fox amdovirus	GFAV	JN202450
Aveparvovirus	**Galliform aveparvovirus 1**	Chicken parvovirus	ChPV	GU214704
		Turkey parvovirus	TuPV	GU214706
Bocaparvovirus	*Carnivore bocaparvovirus 1*	Canine minute virus	CnMV	FJ214110
	Carnivore bocaparvovirus 2	Canine bocavirus 1	CBoV	JN648103
	Carnivore bocaparvovirus 3	Feline bocavirus	FBoV	JQ692585
	Pinniped bocaparvovirus 1	California sea lion bocavirus 1	CslBoV1	JN420361
		California sea lion bocavirus 2	CslBoV2	JN420366
	Pinniped bocaparvovirus 2	California sea lion bocavirus 3	CslBoV3	JN420365
	Primate bocaparvovirus 1	Human bocavirus 1	HBoV1	JQ923422
		Human bocavirus 3	HBoV3	EU918736
		Gorilla bocavirus	GBoV	HM145750
	Primate bocaparvovirus 2	Human bocavirus 2a	HBoV2a	FJ973558
		Human bocavirus 2b	HBoV2b	FJ973560
		Human bocavirus 2c	HBoV2c	FJ170278
		Human bocavirus 4	HBoV4	FJ973561
	Ungulate bocaparvovirus 1	Bovine parvovirus	BPV	DQ335247
	Ungulate bocaparvovirus 2	Porcine bocavirus 1	PBoV1	HM053693
		Porcine bocavirus 2	PBoV2	HM053694
		Porcine bocavirus 6	PBoV6	HQ291309
	Ungulate bocaparvovirus 3	Porcine bocavirus 5	PBoV5	HQ223038
	Ungulate bocaparvovirus 4	Porcine bocavirus 7	PBoV7	HQ291308
	Ungulate bocaparvovirus 5	Porcine bocavirus 3	PBoV3	JF429834
		Porcine bocavirus 4-1	PBoV4-1	JF429835
		Porcine bocavirus 4-2	PBoV4-2	JF429836
Copiparvovirus	**Ungulate copiparvovirus 1**	Bovine parvovirus 2	BPV2	AF406966
	Ungulate copiparvovirus 2	Porcine parvovirus 4	PPV4	GQ387499
Dependoparvovirus	**Adeno-associated dependoparvovirus A**	Adeno-associated virus-1	AAV1	AF063497
		Adeno-associated virus-2	AAV2	AF043303
		Adeno-associated virus-3	AAV3	AF028705
		Adeno-associated virus-4	AAV4	U89790
		Adeno-associated virus-6	AAV6	AF028704
		Adeno-associated virus-7	AAV7	AF513851
		Adeno-associated virus-8	AAV8	AF513852
		Adeno-associated virus-9	AAV9	AX753250
		Adeno-associated virus-10	AAV10	AY631965
		Adeno-associated virus-11	AAV11	AY631966
		Adeno-associated virus-12	AAV12	DQ813647
		Adeno-associated virus-13	AAV13	EU285562
		Adeno-associated virus-S17	AAVS17	AY695376
	Adeno-associated dependovirus B	Adeno-associated virus-5	AAV5	AF085716
		Bovine adeno-associated virus	BAAV	AY388617
		Caprine adeno-associated virus	CapAAV	DQ335246
	Anseriform dependoparvovirus 1	Duck parvovirus	DPV	U22967
		Goose parvovirus-PT	GPV2	JF926695
		Goose parvovirus	GPV	U25749
	Avian dependovirus 1	Avian adeno-associated virus	AAAV	AY186198
	Chiropteran dependoparvovirus 1	Bat adeno-associated virus	BtAAV	GU226971
	Pinniped dependoparvovirus 1	California sea lion adeno-associated virus	CslAAV	JN420372
	Squamate dependoparvovirus 1	Snake adeno-associated virus	SAAV	AY349010
Erythroparvovirus	**Primate erythroparvovirus 1**	Human parvovirus B19-Au	B19V-Au	M13178
		Human parvovirus B19-J35	B19V-J35	AY386330
		Human parvovirus B19-Wi	B19V-Wi	M24682
		Human parvovirus B19-A6	B19V-A6	AY064475
		Human parvovirus B19-Lali	B19V-Lali	AY044266
		Human parvovirus B19-V9	B19V-V9	AJ249437
		Human parvovirus B19-D91	B19V-D91	AY083234
	Primate erythroparvovirus 2	Simian parvovirus	SPV	U26342
	Primate erythroparvovirus 3	Rhesus macaque parvovirus	RhMPV	AF221122
	Primate erythroparvovirus 4	Pig-tailed macaque parvovirus	PtMPV	AF221123
	Rodent erythroparvovirus 1	Chipmunk parvovirus	ChpPV	GQ200736
	Ungulate erythroparvovirus 1	Bovine parvovirus 3	BPV3	AF406967
Protoparvovirus	*Carnivore protoparvovirus 1*	Feline parvovirus	FPV	EU659111
		Canine parvovirus	CPV	M19296
		Mink enteritis virus	MEV	D00765
		Racoon parvovirus	RaPV	JN867610

Table 1.1: The type species for each genus is indicated in bold type. [35]

Genus	Species	Virus or virus variants	Abbr.	ACNO[1]
	Primate protoparvovirus 1	Bufavirus 1a	BuPV1a	JX027296
		Bufavirus 1b	BuPV1b	JX027295
		Bufavirus 2	BuPV2	JX027297
	Rodent protoparvovirus 1	H-1 parvovirus	H1	X01457
		Kilham rat virus	KRV	AF321230
		LuIII virus	LuIII	M81888
		Minute virus of mice (prototype)	MVMp	J02275
		Minute virus of mice (immunosuppressive)	MVMi	M12032
		Minute virus of mice (Missouri)	MVMm	DQ196317
		Minute virus of mice (Cutter)	MVMc	U34256
		Mouse parvovirus 1	MPV1	U12469
		Mouse parvovirus 2	MPV2	DQ196319
		Mouse parvovirus 3	MPV3	DQ199631
		Mouse parvovirus 4	MPV4	FJ440683
		Mouse parvovirus 5	MPV5	FJ441297
		Hamster parvovirus	HaPV	U34255
		Tumor virus X	TVX	In preparation
		Rat minute virus 1	RMV1	AF332882
	Rodent protoparvovirus 2	Rat parvovirus 1	RPV1	AF036710
	Ungulate protoparvovirus 1	Porcine parvovirus Kresse	PPV-Kr	U44978
		Porcine parvovirus NADL-2	PPV-NADL2	L23427
Tetraparvovirus	*Chiropteran tetraparvovirus 1*	Eidolon Helvum (bat) parvovirus	Ba-PARV4	JQ037753
	Primate tetraparvovirus 1	Human parvovirus 4 G1	PARV4G1	AY622943
		Human parv4 G2	PARV4G2	DQ873391
		Human parv4 G3	PARV4G3	EU874248
		Chipmanzee parv4	Ch-PARV4	HQ113143
	Ungulate tetraparvovirus 1	Bovine hokovirus 1	B-PARV4-1	EU200669
		Bovine hokovirus 2	B-PARV4-2	JF504697
	Ungulate tetraparvovirus 2	Porcine hokovirus	P-PARV4	EU200677
	Ungulate tetraparvovirus 3	Porcine Cn virus	CnP-PARV4	GU938300
	Ungulate tetraparvovirus 4	Ovine hokovirus	O-PARV4	JF504699

1.5 Tissue Tropism and Pathogenicity Determinants

Concerning their host range, most parvoviruses, such as MVM, CPV, and FPV, are tightly restricted to their particular hosts. However, some parvoviruses, as for example many of the AAVs, infect human cells by primary attachment to a variety of receptors.

As outlined in section 1.1 (see page 3), two distinct strains of the parvovirus MVM have been described to occur in mice. On one hand, MVMp, the prototype strain, replicates efficiently in mouse fibroblasts [2]. On the other hand, MVMi, the immunosuppressive strain, replicates in T lymphocytes [5]. Both strains display disparate *in vitro* tropism and *in vivo* pathogenicity despite differing by only 14 amino acids in their capsid proteins

---

[1]NIH GenBank accession number

[113]. Beyond that, MVMp and MVMi are serologically indistinguishable, bind to sialic acid and are internalized in both fibroblasts and lymphocytes [114]. Consequently, it could be demonstrated that both viruses propagate in hybrids of the two cell types [115].

In order to map the allotropic determinant of MVM, chimeric viral genomes were constructed *in vitro* from infectious genomic clones of both strains. By mutagenesis and selective plaque assays, the major determinants for the acquisition of fibrotropism for MVMi have been mapped to the capsid gene [116, 117, 113], in particular to the VP2 residues 317 and 321 [118, 119]. Both residues are located at the base of the threefold spike of the virion [120, 121, 116]. Interestingly, these two VP2 residues structurally localize nearby some of the important amino acids determining CPV, FPV, and PPV host range [122, 123, 124]. Further residues (VP2 residues 399, 460, 553, and 558) were identified in MVMi to be able to confer fibrotropism to forward second-site mutants when either residues 317 or 321 are mutated. Those residues cluster around the twofold dimple-like depression [125]. In contrast, the switch to lymphotropism for MVMp is more complex and requires both an equivalent region of the major MVMi capsid protein gene VP2 and a segment of the nonstructural protein genes [117].

MVMi appears to be more pathogenic for mice than MVMp. Oronasal inoculation of MVMi in most neonatal mice was either lethal or resulted in severe growth-retardation in survivors [126], as observed for other parvoviruses (see section 1.4.1, page 5). Whereas MVMp infection was asymptomatic [127], MVMi infection in newborn mice of some inbred strains caused renal papillary hemorrhage and viral replication in endothelia [128], hematopoietic precursors [129], and neuroblasts [130]. Following in utero inoculation of MVMi or MVMp into developing embryo, a broad set of cell types was infected that partially overlapped. Nevertheless, the tissue tropism of MVMp for fibroblasts and of MVMi for endothelium, as well as the higher virulence of MVMi was preserved [131]. By reason of the complexity of MVMi pathogenesis in the neonatal mouse, a more adequate model was required to investigate the virulence of MVMi *in vivo*.

Severe combined immunodeficiency (SCID) mice [132] represent such a model since they lack an antigen-specific immune response, thus allowing the study in adult mice and circumventing the complex situation of heterogenous viral multiplication in embryonic developing tissue. MVMi infection of adult SCID mice gave rise to the suppression of long-term repopulating hemopoietic stem cells in the bone marrow [133], leading to an acute lethal leukopenia and accelerated erythropoiesis [134]. In addition, it has been reported that MVMp evolved in intravenously inoculated SCID mice. Different variants, isolated from single plaques, carried only one of three single amino acid changes at position 325, 362, or 368 in the major VP2 capsid protein. These variants sustained their fibrotropism *in vitro*, but unlike MVMp, they propagated in mouse tissues following

oronasal inoculation, eventually causing death [135, 136]. Two of the three invasive fibrotropic MVMp strains, I362S and I368R, were shown to induce lethal leukopenia in oronasal inoculated SCID mice. Emerging viral populations in leukopenic mice displayed altered sequences in the MVMi genotype at position 321 and 551 of VP2 for infections with the I362S variant or changes at position 551 and 575 in the K368R virus infections. In general, a high level of genomic heterogeneity in the DNA sequence encoding the VP2 protein was observed that clustered at the twofold depression of the viral capsid [137].

Significantly, the amino acids determining *in vitro* tropism (317 and 321), *in vivo* pathogenicity (325, 362, and 368), conferring fibrotropism on MVMi (399, 460, 553, and 558), and those involved in the development of leukopenia (321, 551, and 575) were found to be located on, or near the viral surface. Structurally, these residues cluster mainly by raised elements around the twofold axes of symmetry, in close vicinity of the sialic acid binding pocket [135, 137].

Differences in the tissue tropisms and the pathogenic phenotypes have also been mapped to the capsid proteins of Aleutian mink disease parvovirus [138], porcine parvovirus (PPV) [139], CPV [140, 141], and FPV [142] in a capsid region analogous to that observed for MVM (reviewed in [143]). These pronounced *in vitro* tropism and *in vivo* pathogenicity disparities between the highly homologous viruses might occur at various stages of the infectiuos viral life cycle, including cell receptor binding, virus internalization, uncoating, DNA replication or transcription. Although the same structural element of viruses is involved in mediating host and tissue tropisms, each appears to be affecting a different mechanism. Host ranges of CPV and FPV are controlled by receptor binding, whereas the cell tropisms of MVM appear to be due to restrictions of interactions with intracellular factors [125, 144, 114]. For MVM it was suggested that the point of restriction appeared after nuclear targeting and conversion of genomic ssDNA to RF intermediates but prior to viral genome replication. Most likely, the restraint occurs due to a block in uncoating [145, 146].

As discussed in this section the functional regions among the subfamily *Parvovirinae* co-localize to similar surface regions albeit three general parvovirus topology groups with characteristic local capsid surface differences emerged (see section 1.2, page 3). A profound understanding of functional domains that are involved in fundamental steps of the viral life cycle, particularly receptor attachment, *in vitro* tropism, *in vivo* pathogenicity, and antigenicity are essential for infection and disease control. Hence, showing great promise to allow genetic engineering of parvovirus capsids for the therapeutic delivery to be controlled or modified in gene therapy applications and to develop foreign antigens [144, 143].

1.6 Structure

1.6.1 Parvoviruses in general

Parvovirus capsids are devoid of a lipid envelope and have an average diameter of 18 to 26 nm. The viral capsid is made up of 60 copies of between two and four structural proteins that overlap each other. For each virus there is one major capsid protein present in the capsid structure. Minor proteins form the same core structure, but differ in the sequence length on their amino termini. The capsid proteins display a T=1 icosahedral symmetry and are variously designated VP1-VP4. Thus, the capsid has a 5-3-2 point group symmetry containing 31 rotational symmetry elements that intersect at the center: six fivefolds, ten threefolds, and fifteen twofolds. Despite the differences in protein forms and the low homology between some of the viruses, several structural elements on the capsid surface are common to most parvoviruses. These include raised cylindrical channels at the fivefold axes surrounded by depressed, canyon-like regions. Further shared surface characteristics are protrusions at the threefold axes, termed as spikes or peaks, and dimple-like depressions at the icosahedral twofold axes. A common feature of parvoviruses is their high resistance to physicochemical challenges. This stability provides an effective protection to the fragile, condensed genome in the extracellular environment ensuring transmission between their hosts. The ssDNA genome consists of approximately 5000 bases, packed as either a positive or, more usually, as a negative sense strand. At the 5' and 3' ends, the genome harbors palindromic sequences of about 120 to 250 nucleotides, that form secondary hairpin structures which are essential for the initiation of viral genome replication [147, 148, 149, 125, 150, 151, 144].

1.6.2 MVM

Both DNA-containing full and empty particles were crystallized in the monoclinic space group C2. Following data processing and refinement, the resulting electron density map was interpreted with respect to the amino acid sequence of MVMi. The known CPV structure was used as a phasing model since 52 % of the 587 amino acids in VP2 of MVM are identical to CPV. The polypeptide chain of the major structural protein, VP2, could be traced from residue 39 to residue 587 at the C-terminus [152]. The common c-terminal part of the structural proteins has an eight-stranded antiparallel β-barrel topology, frequently found in viral capsid proteins [153]. Large loops between the β-strands of the β-barrel that form the principal surface features, particularly the threefold spikes, and determine host-range tropism were found to be quite dissimilar in MVM and CPV. The first 37 amino acids are not visible in the electron density

map. Since the N-VP2 terminal part contains a predominantly poly-glycine conserved sequence, it might be highly flexible. In virions, but not in empty capsids, there is weak density extending along the fivefold channels that was modeled as the glycine-rich N-terminal region [154, 155]. *In vitro*, trypsin digestion of full MVM virions results in a truncated VP3 polypeptide that still contains the glycine-rich sequence. In this way, most VP2 N-termini can be cleaved. These findings suggest that there is a dynamic situation at the fivefold channel. In one model, one in five amino termini are externalized along the fivefold axes and are accessible for cleavage. Newly created, cleaved N-VP3 termini could withdraw into the virion and be replaced at the surface by an uncleaved N-VP2 terminus. [156, 125]. A substantial amount of internal electron density could be related to 10 DNA nucleotides that were previously found in the analysis of the structure of CPV [157, 158]. For MVM, 19 additional DNA nucleotides were identified in a difference electron-density map with respect to the data of empty particles. Thus, 29 ordered, or partially ordered, nucleotides per icosahedral asymmetric unit imply that approximately 34 % of the total genome display icosahedral symmetry. This finding, and the conservation of base-binding sites between MVMi and CPV, identifies a DNA-recognition site on the parvoviral capsid interior [125].

1.7 Nucleic Acid

1.7.1 Genome organization

1.7.2 Transcriptome

1.8 Viral proteins

1.8.1 Structural Proteins

Three capsid proteins (LRV) [159] Three capsid proteins (AAV) [160, 161]

1.8.2 Non-structural proteins

1.9

1.9.1

1.9.2

2 Methods

2.1 Cell Cultures

A9 ouab[r]l1 cells, a derivative from the original HGPRT[-] L-cell line A9 represent a clone resistant to 10^{-3} M ouabain after nitrosoguanidine mutagenesis [162]. NB324K cells are a clone of SV40-transformed human newborn kidney cells [163]. The SV40 large T antigen was detected by immunofluorescent staining with monoclonal antibodies [164]. However, NB324K cells do not produce infectious SV40 spontaneously. Both cell lines, A9 mouse fibroblasts and NB324K cells, were routinely propagated under a minimal number of passages in DMEM supplemented with 5 % of heat inactivated fetal bovine serum at 37 ℃ in 5 % CO_2 atmosphere.

2.1.1 Freezing and thawing of cells

Before use the A9 mouse fibroblasts or NB324K cells were thawed at 37 ℃ and cultured in 5 mL of pre-warmed DMEM supplemented with 5 % FCS. The medium was replaced every 3 to 4 days. In order to freeze the cells for long storage in liquid nitrogen they were passed the day before, to ensure exponential growth. Subsequently, 7.5 % DMSO was added and the cells were frozen slowly at -70 ℃ over night before transfer to liquid nitrogen.

2.2 Virus Stocks

Stocks of MVM without detectable levels of VP3 were propagated on A9 mouse fibroblast monolayers. As soon as the cytopathic effect became evident, the supernatant was collected and pre-cleared from cell debris by low-speed centrifugation. Thereby, intracellular, VP3 rich capsids were discarded. In order to remove low-molecular contaminants, virus containing SN was pelleted through 20 % sucrose cushion in PBS by ultra-centrifugation. Virus titers were determined by qPCR as DNA-packaged particles per microliter.

2.2.1 Separation of empty and full capsids

Sucrose purified capsids were prepared as previously described in section 2.2, page 17. The virus pellet was resuspended in 10 mL PBS. Caesium chloride was added to a density of 1.38 g/mL adjusted by refractometry (η=1.371) at 4 ℃. The gradient was centrifuged to equilibrium for 24 h at 41000 rpm and 4 ℃ in a Beckmann SW-41 Ti rotor. Gradients were fractionated and tested for intact capsids by dot blot analysis using B7 mAb. CsCl was depleted from the corresponding fractions by size-exclusion chromatography through PD-10 desalting columns and the capsids were concentrated in Amicon® centrifugal filter devices when required.

2.3 Freezing bacteria stocks in glycerol

Bacteria were frozen in dry ice. A volume of 700 μL of the bacteria culture that was grown over night in LB-medium was mixed with 300 μL of 50 % glycerol in a cryotube. In order to mix well the glycerol the cryotube was vortexed intensively. Following snap-freeze in dry ice the bacteria were stored at -70 ℃.

2.4 Anion-exchange chromatography

A Mono Q HR 5/5 (Pharmacia) column (5 x 50 mm) was used to analyse viral samples. The Mono Q column was connected to the ÄKTAmicro chromatography system (GE Healthcare) that was operated by the UNICORN control software. The Mono Q column was equilibrated with six column volumes (CV) starting buffer (20 mM Tris-HCl, 1 mM EDTA, pH 7.2). Samples (1 mL) containing at least 10^{10} virus particles in 10 mM Tris-HCl, 1 mM EDTA, pH 8 were applied to the Mono Q column trough a 2 mL loop. After eluting the protein, which did not bind to the column in the starting buffer, a linear salt gradient (0-2 M NaCl) in 20 mM Tris-HCl, 1 mM EDTA, pH 7.2, was applied. Fractions of 0.185 mL were collected in 96-well plates. Viral genomes in each fraction were quantified by qPCR.

Occasionally, the Mono Q column needed to be washed. Increased back-pressure, colour change at the top of the column, decreased sample recoveries, or loss of resolution indicates that the column matrix requires regeneration. In order to circumvent such problems, the column was washed every tenth run. To eluate contaminants that tightly stick to the column the following harsh conditions were applied to the reversed (bottom to top) Mono Q column. 500 μL 2 M NaCl solution was injected and subsequently, the column was rinsed with water. Then, 500 μL 2 M NaOH solution was injected and the column was rinsed with water. Finally, 500 μL 75 % acetic acid was injected before the

column was re-equilibrated with starting buffer.

All buffers were filtered and degassed before application to the Mono Q column.

2.5 Quantitative PCR

Amplification of MVM DNA and real-time detection of PCR products were performed by using BioRad CFX96 technology with SYBR green supermix. PCR was carried out by using the hot-start iTaq™ DNA polymerase (Bio-Rad Laboratories) following the manufacturer's guide-lines. Viral DNA was isolated using DNeasy blood and tissue kit. Elution of the purified vDNA was carried out using 100 μL elution buffer. As templates 2 μL of the isolated viral DNA were used for the PCR reaction and were added to the following master mix:

Component	Amount	Final concentration
dH$_2$O, PCR grade	6 μL	-
Forward primer, 10 pM	1 μL	0.5 pM
Reverse primer, 10 pM	1 μL	0.5 pM
2x IQ™ SYBR® Green Supermix	10 μL	1x
Total volume	**18 μL**	

Table 2.1: Master mix for quantitative PCR. In order to minimize pipetting errors a master mix was prepared. Following preparation the master mix was distributed across the 96 well plates. The master mix contains all the ingredients which are required for the DNA amplification except the initial DNA template that differs among the samples.

To ensure accurate quantification, the 96-well plates containing master mix and template DNA were shortly spun and transferred into the BioRad CFX96 unit. The following PCR program was used for quantification of viral DNA:

Cycles	Step	Temperature	Time
1x	Initial denaturation	95 ℃	300 s
40x	Denaturation	95 ℃	15 s
	Annealing	61 ℃	15 s
	Extension	72 ℃	15 s
1x	Final denaturation	95 ℃	60 s
1x	Melting curve	65 ℃ up to 95 ℃	0.1 ℃/s

Table 2.2: PCR conditions for the amplification and real-time detection of MVM DNA.

To provide standards for sample quantification, serially diluted plasmids containing the entire MVM genomic DNA were used. For cell number variations that may exist between

the samples, the number of applied cells per PCR reaction needed to be quantified for normalization as well. For this purpose quantification of cellular β-actin gene was performed. After normalization, direct comparison of the results is possible. β-actin quantification was carried out with the same PCR conditions outlined in table 2.2, 19.

2.6 Immunoprecipitation

Either *in vitro* treated viruses or viruses from cell extracts were transferred to LoBind tubes that were pre-blocked with PBS containing 1 % bovine serum albumin (PBSA 1 %). The volume was adjusted to 200 μL with PBSA 1 %. The antibody was added in excess and incubated with the viral capsids for 1 h at 4 ℃ on a rotary shaker. Subsequently, 20 μL protein G-agarose beads were added. Following overnight incubation at 4 ℃ and centrifugation at 2500 rpm for 5 min the supernatant was discarded. The beads were washed 4 times with PBSA 1 %. To remove the BSA an additional wash step was carried out with PBS. Finally, the beads were frozen at -20 ℃ until further use or immediately processed.

2.7 SDS-PAGE and Western blotting

Immunoprecipitated capsids were dissolved in 20 μL protein loading buffer (reference) containing 2 % SDS and 10 % glycerol. The samples were boiled at 96 ℃ for 8 min. Viral proteins were separated through a NuPAGE® 10 % Bis-Tris Gel (Invitrogen). The XCell Sure Lock™ Electrophoresis Cell (Invitrogen) was used to separate the proteins. The gel was first run at 30 V for 10 min to stack the proteins. In this way, sharper bands could be achieved. Separation of the different proteins was accomplished at 200 V. Following separation, the proteins were blotted on a methanol activated, porous, 0.2 μm polyvinylidene fluoride (PVDF) Immobilon® Transfer Membrane (EMD Millipore). Blotting was carried out at 30 V for 1 h 10 min using XCell II™ Blot Module (Invitrogen). The membrane was blocked in TBS-T buffer (reference) supplemented with 5 % milk overnight at 4 ℃. Subsequently, the membrane was probed with a polyclonal rabbit antibody against linear MVM-VP epitopes that was diluted 1:2000 in 3 mL TBS-T containing 1 % milk. The first antibody (reference) was incubated for 1 h at RT. The PVDF membrane was washed in TBS-T for a total 90 min with many buffer replacements. Subsequently, the horseradish peroxidise conjugated secondary antibody (goat α-rabbit-HRP, reference) was added for 1 h at RT. This secondary goat anti-rabbit antibody was diluted 1:20000 in TBS-T supplemented with 1 % milk. To deplete remaining antibodies, the membrane was washed in the same way as described above except for a final wash step with TBS (reference). VP1, VP2, and possibly VP3 were visualized by a

chemiluminescence system (SuperSignal West Dura Extended Duration Substrate, reference) following the manufacturer's instructions. Following this treatment, the PVDF membrane was exposed to a film (Amersham Hyperfilm™ ECL, reference). Finally, the film was developed using Anatomix Developer Replenisher Solution and Fixer and Replenisher Solution (reference).

2.8 Chymotrypsin treatment

Virus particles were incubated with 0.5 mg/mL chymotrypsin (Sigma) in PBS for 1.5 h at 37 ℃. The reaction was stopped by adding 100 μM chymostatin (Sigma). Negative controls were incubated in the same buffer for the same time.

2.8.1

2.9

2.9.1

2.9.2

Part II

Publication

1 Wolfisberg et al., Journal of Virological Methods, 2013

Impaired genome encapsidation restricts the *in vitro* propagation of human parvovirus B19.

Raphael Wolfisberg, Nico Ruprecht, Christoph Kempf and Carlos Ros

Impaired genome encapsidation restricts the *in vitro* propagation of human parvovirus B19

Raphael Wolfisberg[a], Nico Ruprecht[a], Christoph Kempf[a,b], Carlos Ros[a,b,*]

[a] Department of Chemistry and Biochemistry, University of Bern, Freiestrasse 3, 3012 Bern, Switzerland
[b] CSL Behring AG, Wankdorfstrasse 10, 3000 Bern 22, Switzerland

ABSTRACT

The lack of a permissive cell culture system hampers the study of human parvovirus B19 (B19V). UT7/Epo is one of the few established cell lines that can be infected with B19V but generates none or few infectious progeny. Recently, hypoxic conditions or the use of primary CD36+ erythroid progenitor cells (CD36+ EPCs) have been shown to improve the infection. These novel approaches were evaluated in infection and transfection experiments. Hypoxic conditions or the use of CD36+ EPCs resulted in a significant acceleration of the infection/transfection and a modest increase in the yield of capsid progeny. However, under all tested conditions, genome encapsidation was impaired seriously. Further analysis of the cell culture virus progeny revealed that differently to the wild-type virus, the VP1 unique region (VP1u) was exposed partially and was unable to become further externalized upon heat treatment. The fivefold axes pore, which is used for VP1u externalization and genome encapsidation, might be constricted by the atypical VP1u conformation explaining the packaging failure. Although CD36+ EPCs and hypoxia facilitate B19V infection, large quantities of infectious progeny cannot be generated due to a failure in genome encapsidation, which arises as a major limiting factor for the *in vitro* propagation of B19V.

© 2013 Elsevier B.V. All rights reserved.

1. Introduction

Human parvovirus B19 (B19V) is spread worldwide and typically causes a mild self-limiting infection in children known as *erythema infectiosum*. B19V has also been associated to myocarditis, acute and chronic arthropathies in adults, transient aplastic crisis and chronic anemia in individuals with altered immunologic or hematologic conditions, hydrops fetalis and intrauterine fetal death (Heegaard and Hornsleth, 1995; Heegaard and Brown, 2002; Servey et al., 2007).

Considering its worldwide distribution, prevalence and associated disorders, B19V is regarded as a prominent human pathogen and the only parvovirus undoubtedly linked to human disease. However, the experimental research with B19V is hampered seriously due to the lack of an appropriate and sufficiently permissive cell system to propagate the virus and study its biology. The reason for this is the rigorous replication requirements of the virus. B19V has an extraordinary tropism for erythroid progenitor cells in the bone marrow at a particular differentiation stage corresponding to BFU-E and CFU-E (Takahashi et al., 1990; Ozawa et al.,

1986, 1987). The narrow tropism of B19V is mediated, at least in part, by its particular uptake mechanism. B19V utilizes globoside (Gb4Cer) as a primary attachment receptor, which is expressed in few cell types (Brown et al., 1993) and a co-receptor (Weigel-Kelley et al., 2003) to initiate the internalization process. However, cells expressing the required receptors and co-receptors are not always permissive, suggesting that the selective replication of B19V is determined by additional intracellular factors restricted to erythroid cells (Pallier et al., 1997; Brunstein et al., 2000; Gallinella et al., 2000; Guan et al., 2008; Chen et al., 2010; Luo et al., 2011). The high viremia that is typically associated to B19V acute infections, exceeding occasionally 10^{13} genome equivalents (geq) per ml of plasma (Kooistra et al., 2011), suggests that the virus can replicate efficiently in the target cells when all the required elements are present. However, despite continuous efforts, the specific cellular factors that control B19V infection in the natural target cells have not yet been reproduced adequately in an established cell line. Some erythropoietin-dependent leukemic cell lines, notably UT7/Epo (Shimomura et al., 1992) and KU812Ep6 (Miyagawa et al., 1999), have been shown to be semi-permissive to B19V infection, producing in general none or minor amounts of infectious progeny. The permissivity of non-erythroid cells, such as HepG2 cells has produced contradictory results (Caillet-Fauquet et al., 2004a; Bonvicini et al., 2008). Considering all these limitations, highly viremic donors without B19V neutralizing antibodies remain the only source of infectious B19V. Thus, the need to develop

* Corresponding author at: Department of Chemistry and Biochemistry, University of Bern, Freiestrasse 3, 3012 Bern, Switzerland. Tel.: +41 31 6314349; fax: +41 31 6314887.

E-mail address: carlos.ros@ibc.unibe.ch (C. Ros).

a cell culture method capable of producing large amounts of infectious B19V remains a major challenge.

Recently, the use of cells cultured under hypoxic conditions has been described as a promising method to produce high quantities of infectious particles (Caillet-Fauquet et al., 2004b; Pillet et al., 2004; Chen et al., 2011). Similarly, the use of *ex vivo* expanded CD36+ primary human erythroid progenitor cells (CD36+ EPCs), previous CD34+ *in vitro* preselection (Pillet et al., 2008; Wong et al., 2008), has also been described as a highly permissive system, based on the expression of B19V non-structural and capsid proteins. A simplified approach to generate CD36+ EPCs directly from ordinary blood samples, without *ex vivo* stem cell mobilization has been reported (Filippone et al., 2010). The combination of both approaches, primary CD36+ EPCs cultured under hypoxic conditions, has been shown to enhance remarkably B19V infection (Chen et al., 2011). Hypoxia, which mimics the oxygen microenvironment in the bone marrow, seems to promote B19V infection by the direct stimulating effect of HIF1α on the B19V p6 promoter (Pillet et al., 2004). However, an alternative HIF1α-independent mechanism based on STAT5A and MEK signaling has been proposed recently (Chen et al., 2011).

These novel approaches based on hypoxia and primary CD36+ EPCs have been compared systematically in infection and transfection experiments with the established erythroid cell line UT7/Epo. In all cases, a substantial amount of capsid progeny was obtained. The use of the novel approaches resulted in a significant acceleration of the infection and the augmentation in the number of infected cells resulting in a modest but noticeable increase in virus progeny production. However, in all tested cells and under all conditions genome encapsidation was impaired seriously generating an empty non-infectious virus progeny. Differently to the wild-type virus, the VP1 unique region (VP1u) of the virus progeny was exposed partially and upon heat treatment did not undergo the expected conformational change that renders VP1u fully externalized. The abnormal configuration and rigidity of VP1u, which utilizes the genome encapsidation portal for its externalization, might constrict the fivefold axes channel impeding the translocation of the viral genome into the pre-assembled capsid.

2. Materials and methods

2.1. Cells and viruses

UT7/Epo cells were maintained in Eagle's minimum essential medium (MEM) supplemented with 5% heat-inactivated fetal calf serum (FCS) and 2 U/ml of recombinant human erythropoietin (Epo; Janssen-Cilag, Midrand, South Africa) at 37 °C with 5% CO$_2$. For hypoxic conditions the oxygen tension was lowered to 1%. Cells with adherent phenotype were selected by removing the non-adherent cells in every passage. CD36+ erythroid progenitor cells (CD36+ EPCs) were obtained from ordinary blood samples and cultured as described previously (Filippone et al., 2010). A B19V-infected plasma sample (Genotype 1; CSL Behring AG, Charlotte, NC), without detectable B19V-specific IgM or IgG antibodies, was used as a source of native infectious virus. The virus was pelleted by ultracentrifugation through 20% (w/v) sucrose and the concentration of virions was determined by quantitative PCR (qPCR).

2.2. Antibodies and chemicals

Two human monoclonal antibodies (mAb), one directed to a conformational epitope in the major capsid protein VP2 (mAb 860-55D), which detects exclusively intact capsids, and the other against the N-terminal region of VP1, also known as VP1 unique region (VP1u) (mAb 1418), were provided by S. Modrow

(Regensburg, Germany). These antibodies were produced from peripheral blood mononuclear cells of normal, healthy individuals with high titers of serum antibodies against B19 virus proteins (Gigler et al., 1999). A rabbit antibody against the C-terminal region of VP1u was described earlier (Bönsch et al., 2008). A mouse mAb against B19V capsids (mAb 521-5D) was purchased from Millipore (Billerica, MA). A globoside-specific mouse IgM mAb (AME-2) was provided by J. de Jong (The Netherlands Red Cross, Amsterdam, Netherlands). Mouse IgG mAb against Ku80 and CD49e were purchased from BD Biosciences (San Jose, CA). A mouse antibody against B19V proteins was obtained from US biologicals (Swampscott, MA). Chloroquine diphosphate (CQ) was purchased from Sigma (St. Louis, MO) and dissolved in water.

2.3. Flow cytometry

The presence of B19V receptors and co-receptors on the cell surface of UT7/Epo cells was analyzed quantitatively by flow cytometry. UT7/Epo cells were incubated with either an anti-Ku80 or an anti-Gb4Cer antibody at 4 °C for 1 h in PBS containing 2% fetal calf serum, followed by incubation with fluorescein isothiocyanate (FITC)-conjugated rat anti-mouse IgG or IgM, respectively (BD Biosciences). Additionally, UT7/Epo cells were stained with R-phycoerythrin conjugated anti-human CD49e (BD Biosciences). The cells were analyzed on a BD FacsCanto II (Becton Dickinson, San Jose, CA). Data acquisition and analysis were conducted with a software (BD FacsDiva, BD Biosciences).

2.4. Infection

UT7/Epo and primary CD36+ EPCs (3×10^5) cultured under normoxia or hypoxia (1% O$_2$) during 2 days, were infected with B19V at 10^4 geq per cell for 1 h at 4 °C. The cells were washed to remove unbound viruses and further incubated at 37 °C. At different post-infection (p.i.) times, cells and supernatants were collected. The cells were washed and processed for immunofluorescence (IF), immunoprecipitation (IP), as well as DNA and RNA extraction. The supernatant was used for IP and DNA extraction.

2.5. Transfection

A total of 5×10^6 UT7/Epo cells, cultured under normoxia or hypoxia (1% O$_2$) during 2 days, were transfected using the AMAXA nucleofector^{TM} II device (Lonza, Cologne, Germany) following the manufacturer's instructions. Transfection was carried out with 5 μg of the B19V genome excised from a B19V infectious clone (pB19-M20) (Zhi et al., 2004) or with 2 μg of a GFP-control plasmid, using the T-20 program. As a transfection reagent, AMAXA^{TM} Cell Line Nucleofector^{TM} Kit R (Lonza) was used. After transfection, the cells were maintained in 20 ml of pre-warmed culture medium. A volume of 5 ml of fresh MEM culture medium supplemented with 5% FCS and Epo (2 U/ml) was added to the cells 24 h post-transfection (p.t.). At increasing times p.t., the cells and supernatant were collected for further analysis.

2.6. Quantitation of B19V DNA and NS1 mRNA

Total DNA was extracted from cells or from the supernatant by using the DNeasy blood and tissue kit (Qiagen, Valencia, CA). For the isolation of total mRNA, cells were transferred to RNase-free tubes (Safe-Lock Tubes 1.5 ml, Eppendorf Biopur) and washed twice with PBS. Total poly-A-mRNA was isolated with the Dynabeads mRNA direct kit (Roche Diagnostics, Mannheim, Germany). The RNA preparations were used for reverse transcription as described previously (Bönsch et al., 2010a). Amplification of DNA or cDNA and real-time detection of PCR products were performed by qPCR

with the iQ SYBR Green Supermix and the CFX96 device (Bio-Rad, Cressier, Switzerland). Primers used for amplification were described elsewhere (Bönsch et al., 2010a).

2.7. Immunoprecipitation of B19V particles and quantitation of virions

Viral particles were immunoprecipitated from cell extracts or from the supernatant of infected cells with a human mAb against intact capsids (860-55D) (Gigler et al., 1999). As reference control, a known amount of virions was added to the uninfected cell extracts or to the supernatant. After overnight incubation at 4 °C in the presence of 20 μl of protein G agarose beads (Santa Cruz Biotechnology, Heidelberg, Germany) the supernatant was discarded and the beads were washed four times with PBSA. Immunoprecipitated viral capsids were detected by SDS-PAGE. To verify the presence of the viral genome, DNA was extracted from the immunoprecipitated virions by using the DNeasy blood and tissue kit (Qiagen) and quantified as specified above.

2.8. Immunofluorescence

Cells or purified viruses were fixed on coverslips by using acetone/methanol (1:1 [v/v]) solution at −20 °C for 4 min. Following blocking with goat serum diluted in PBS (20% [v/v]), the samples were incubated with the primary antibodies in PBS containing 2% goat serum for 1 h at room temperature (RT). The samples were washed and the appropriate fluorescently labeled secondary antibody in 2% goat serum was added for 1 h at RT. Nuclei was stained with 4′,6-diamidino-2-phenylindole (DAPI). Mowiol supplemented with 2.5% 1,4-Diazabicyclo[2.2.2]octan (DABCO) was used to maintain the fluorescent signal. Samples were examined by confocal laser scanning microscopy (Axiovert 200M, Carl Zeiss A.G., Feldbach, Switzerland).

2.9. Fluorescence in situ DNA hybridization

The presence of newly replicated viral genomes in the infected cells was examined by fluorescence in situ DNA hybridization (FISH). Biotinylated probes specific for B19V DNA were generated from PCR products by nick translation (Roche), according to the manufacturer's instructions. The size of the hybridization probes was 200–500 nucleotides in length, as confirmed by agarose gel electrophoresis. Cells were fixed and immunostained with mAb 860-55D against capsids and incubated in a humid chamber at 37 °C for 18 h with a volume of 20 μl hybridization mix (5 ng/μl biotinylated probe in 60% deionised formamide, 300 mM NaCl, 20 mM sodium citrate, 10 mM EDTA, 25 mM NaH$_2$PO$_4$ pH 7.4, 5% dextran sulfate and 250 ng/μl sheared salmon sperm DNA). Subsequently, the cells were washed (50% deionized formamide, 25 mM NaCl and 2.5 mM sodium citrate pH 7.4) three times for 5 min at RT and once at 37 °C. The samples were blocked for 30 min with 1% blocking solution (Roche) in 150 mM NaCl, 100 mM Tris–HCl pH 7.4. Biotin was detected with avidin-rhodamine (Roche) 1:500 in blocking solution for 45 min. Finally, the cells were washed three times 10 min (200 mM Tris–HCl pH 7.4, 1.5 M NaCl and 0.05% Tween-20), mounted with mowiol supplemented with DABCO and examined by confocal laser scanning microscopy.

3. Results

3.1. General profile of B19V infection in UT7/Epo cells

UT7/Epo cells have been used extensively to study B19V infection. However, intracellular factors restrict severely the infection of B19V in these and other cells, resulting in the production of none or few infectious progeny (Pallier et al., 1997; Brunstein et al., 2000; Gallinella et al., 2000; Guan et al., 2008). In order to better identify which steps of the infection are deficient, different parameters of B19V infection in UT7/Epo cells have been analyzed. Analysis of the expression profile of B19V receptor and co-receptors over a period of six weeks showed a high and stable expression of Gb4Cer and CD49e along the specified period. In contrast, expression of Ku80, which may have a similar role to Gb4Cer in certain cells (Munakata et al., 2005), was not significant (Fig. 1A). IF microscopy examination of infected cells confirmed that B19V can attach and internalize cells, adopting the typical intracellular distribution around the microtubule organizing center (MTOC) observed in other parvovirus infections (Fig. 1B). The kinetics of viral transcription and replication were analyzed quantitatively. The synthesis of viral RNA (NS1 mRNA) was already detectable by 3 h p.i. and reached a plateau by 24 h p.i. (Fig. 1C). Viral replication started later and reached a plateau by the third day p.i. (Fig. 1D). Expression of viral proteins became detectable after 24 h and reached a plateau after 2 days (Fig. 1E). Immunoprecipitation at 3 days p.i. with an antibody against intact viral particles (mAb 860-55D) (Gigler et al., 1999) demonstrated that virus assembly occurred and that a significant amount of capsid progeny was produced (Fig. 1F). Quantitative determination of the viral DNA from the immunoprecipitated capsids revealed that the virus progeny was essentially empty (Fig. 1G). Mature virion progeny was not either detected in the supernatant of the infected cells (Fig. 1H). These results together indicate that despite the substantial amount of capsid progeny produced, deficiencies in genome packaging and capsid egress limit the progression of B19V infection in UT7/Epo cells.

3.2. B19V infection of UT7/Epo cells, under normoxia or hypoxia, generates mostly empty capsids

Infected cells were collected at progressive days, washed and lysed. Viral particles were immunoprecipitated from the cell lysate with the antibody 860-55D, against assembled capsids. The results confirmed that under hypoxic conditions, the capsid progeny was more abundant but also appeared earlier (after 48 h p.i. under normoxia and after 24 h p.i. under hypoxia) (Fig. 2A and B). These results confirmed previous observations indicating that hypoxia enhances B19V infection (Caillet-Fauquet et al., 2004b; Pillet et al., 2004; Chen et al., 2011). The virus progeny generated under hypoxic or normoxic conditions was further characterized. The amount of viral genomes in the immunoprecipitated viral particles from the experiment shown in Fig. 2A and B was analyzed quantitatively. The results revealed that independently of the oxygen environment, a limited number of progeny capsids (<1% of the reference control) contained the viral DNA (Fig. 2C and D). Quantitation of the viral DNA in the supernatant of the infected cells showed no increase over the background signal (day 0 p.i.) under normoxia and modestly under hypoxic conditions (Fig. 2E and F). Capsid proteins in the supernatant were undetectable by IP and Western blot (data not shown). These results indicate that although hypoxic conditions result in the acceleration of the infection and an augmented capsid production, the improvement of the genome encapsidation step was not significant.

3.3. Hypoxia enhances significantly the transfection efficiency, however genome packaging and egress remained restricted

In a control transfection experiment in UT7/Epo cells, the oxygen level did not influence the transfection efficiency with a control plasmid expressing green fluorescent protein (GFP) (Fig. 3A). However, the transfection efficiency increased drastically under hypoxic conditions with an infectious clone of B19V (pB19-M20)
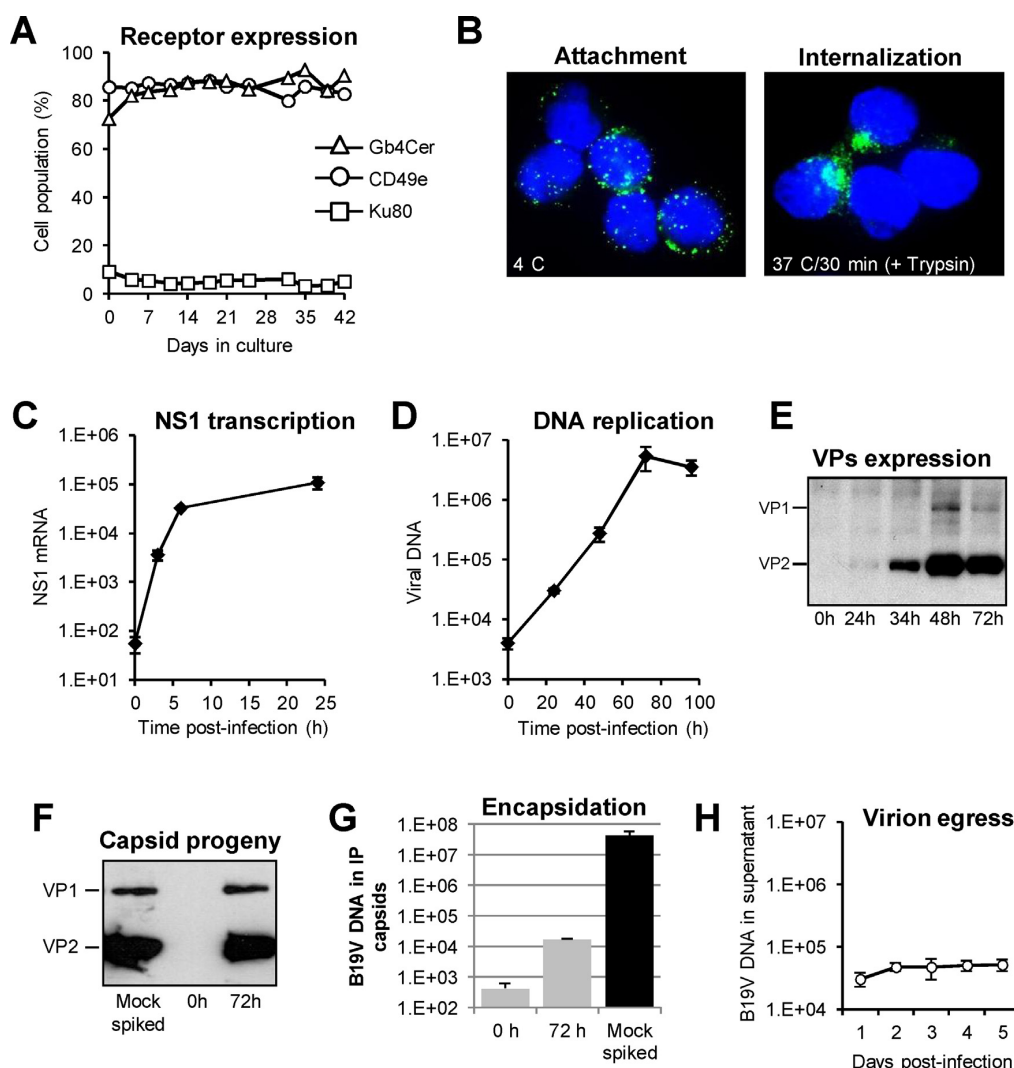
Fig. 1. Characterization of B19V infection in UT7/Epo cells. (A) Expression of B19V-related receptors in UT7/Epo cells. The presence of B19V receptors and co-receptors on the cell surface of UT7/Epo cells was quantitatively analyzed by flow cytometry during a period of 6 weeks. (B) Binding and internalization of B19V in UT7/Epo cells. B19V was added to the cells at 4 °C for 2 h, washed, fixed and stained with an antibody against intact capsids. For internalization, the cells were further incubated for 30 min at 37 °C, washed and trypsinized to remove uninternalized particles. (C) Kinetics of NS1 mRNA synthesis in infected cells. At increasing times p.i., total mRNA was isolated and NS1 mRNA quantified. Samples taken 10 min p.i. served as background controls. (D) Kinetics of viral DNA replication. At increasing times p.i., total DNA was isolated and viral DNA quantified. Samples taken prior to virus internalization served as background controls. (E) Kinetics of B19V capsid proteins expression. (F) Production of assembled capsid progeny in UT7/Epo cells. B19V capsids were immunoprecipitated from cell extracts with mAb 860-55D against intact capsids. As a reference control, B19V (4×10^{10}) was added to mock-infected cell extracts. (G) B19V capsids were immunoprecipitated and B19V DNA was quantified. As a reference control, B19V (4×10^{10} virions) was added to mock-infected cell extracts. (H) Quantitation of virus egress. B19V DNA was quantified from the supernatant of the infected cells.

(Fig. 3B). Immunoprecipitation experiments confirmed that assembled capsids were generated (Fig. 3C) and similarly to the infection experiments, progeny capsids were slightly more abundant and appeared earlier under hypoxic conditions.

As shown in Fig. 3D, at progressive times p.t. no viral DNA above the input signal was detected in the immunoprecipitated capsids. Additionally, virions were not detectable in the supernatant of the transfected cells (Fig. 3E).

3.4. Chloroquine enhances B19V infection in UT7/Epo cells but has no influence in genome encapsidation and egress

It has been shown previously that chloroquine (CQ) enhances B19V infection. In the presence of CQ, an increased production of viral DNA, RNA and proteins was observed and the infection was accelerated (Bönsch et al., 2010b). The production of mature virions in CQ-treated UT7/Epo cells was examined. The results confirmed, that in the presence of CQ, an increased amount of assembled capsids was produced (Fig. 4A). However, similar to untreated cells, most of the progeny capsids remained empty (Fig. 4B). Viral DNA or capsid proteins were not detected in the supernatant of infected cells (data not shown).

3.5. B19V infection is enhanced in CD36+ EPCs, in particular under hypoxia, but genome encapsidation remains restricted

Immunofluorescence microscopy examination of infected primary CD36+ EPCs confirmed that B19V can attach and internalize
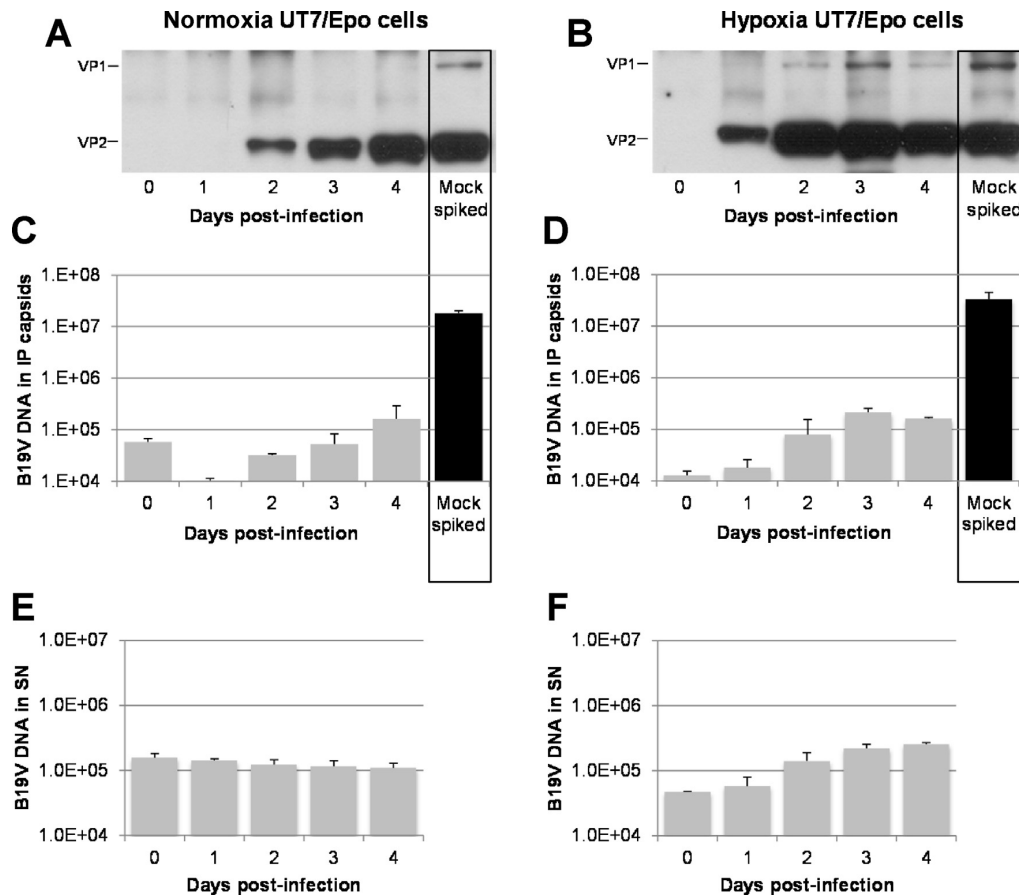
Fig. 2. Capsid progeny and quantitation of virions in UT7/Epo cells. Cells (3×10^5) were infected with B19V under normoxia or hypoxia. At progressive times p.i., the supernatant was collected and the cells were lysed. (A and B) B19V capsids were immunoprecipitated from the cell extracts with mAb 860-55D. As a reference control, B19V (4×10^{10}) was added to mock-infected cell extracts. (C and D) B19V DNA was quantified from the immunoprecipitated capsids. As a reference control, B19V (4×10^{10} virions) was added to mock-infected cell extracts. (E and F) B19V DNA was quantified from the supernatant of the infected cells. Data are the mean ± SD of two independent experiments.

EPCs without noticeable differences to UT7/Epo cells or between normoxic and hypoxic conditions (Fig. 5A). However, the oxygen environment had an important influence in the number of cells infected by B19V. By 2 days p.i., the number of UT7/Epo cells with detectable capsid progeny was 1–5% and 15–20% under normoxia and hypoxia, respectively. In CD36+ EPCs, the number of infected cells increased to approximately 25% under normoxia and above 70% under hypoxic conditions (Fig. 5B).

Immunoprecipitation experiments with the antibody 860-55D (against intact capsids) at progressive days p.i. showed, that regardless the oxygen conditions, progeny capsids appeared earlier in CD36+ EPCs than in UT7/Epo cells. While in UT7/Epo cells, capsid progeny production reached a plateau on day 4 under normoxia and on day 2–3 under hypoxia, in CD36+ EPCs, maximal capsid progeny was observed already after 24 h p.i. (compare Fig. 6A and B and Fig. 2A and B). The amount of viral DNA in the immunoprecipitated samples from the experiment shown in Fig. 6A and B was analyzed quantitatively. The results revealed that a limited number of capsids containing the viral DNA were produced after 24 h p.i. and did not increase subsequently (Fig. 6C and D). The presence of viral DNA in the supernatant increased and reached similarly a plateau already after 24 h p.i. (Fig. 6E and F).

Capsid progeny was detectable in the supernatant of infected EPCs, in particular under hypoxic conditions (Fig. 7A and B).

However, quantitation of their DNA content and comparison with the reference control revealed that only a modest proportion of the particles represented mature infectious virions (Fig. 7C and D). The IP of capsid-associated DNA increased and reached a plateau by 24 h p.i. At this time, the capsid progeny was undetectable under normoxia and hardly detectable under hypoxia (Fig. 7A and B). Therefore, the increase of capsid progeny observed in the following days represented essentially empty particles. These results indicate that despite the augmented and earlier production of virus progeny, the deficient packaging step remains the limiting factor for the propagation of B19V in CD36+ EPCs.

3.6. Intracellular distribution of viral genomes and capsids

The presence and distribution of the viral genomes and capsids in the infected UT7/Epo cells was examined by FISH. In some cells, assembled capsids and viral genomes colocalized within large intranuclear clusters (Fig. 8A, panel i) resembling the nuclear compartments described earlier in AAV, containing non-structural proteins, capsids, and viral genomes and where presumably encapsidation takes place (Hunter and Samulski, 1992; Wistuba et al., 1997). However, in a larger proportion of cells the viral genomes appeared isolated in the nucleus, while the assembled capsids were detected in the cytoplasm (Fig. 8A, panel ii).
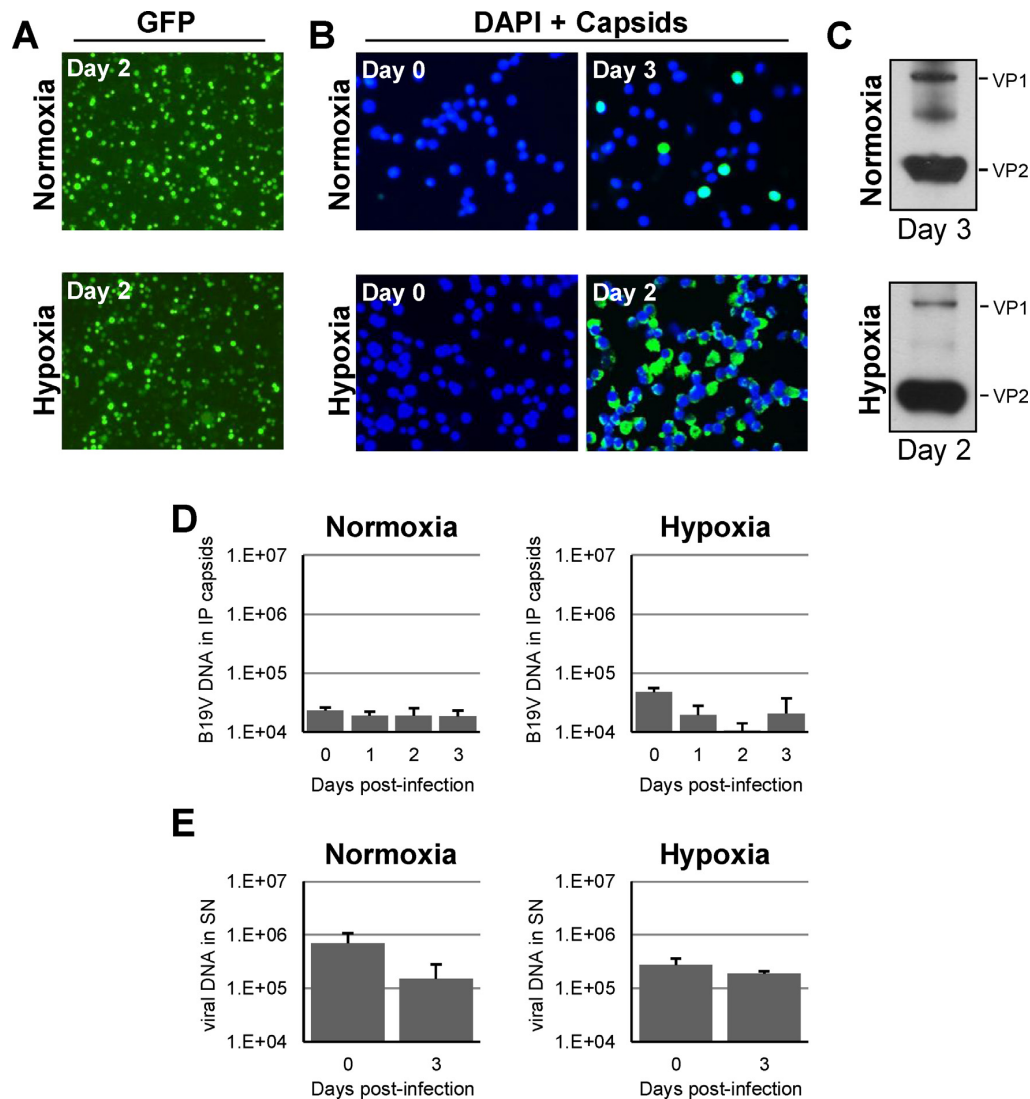
Fig. 3. Transfection of UT7/Epo cells with a B19V infectious clone under normoxia and hypoxia. (A) Transfection of UT7/Epo cells with a control plasmid expressing GFP is not influenced by normoxia or hypoxia. (B) Detection of B19V capsids by IF following transfection with a B19V infectious clone (pB19-M20). (C) Detection of B19V capsids by IP with mAb 860-55D from pB19-M20 transfected cells. (D) At progressive days p.i. B19V capsids were immunoprecipitated from cell lysates and B19V DNA was quantified. (E) B19V DNA was quantified from the supernatant of the infected cells. Data are the mean ± SD for two independent experiments.
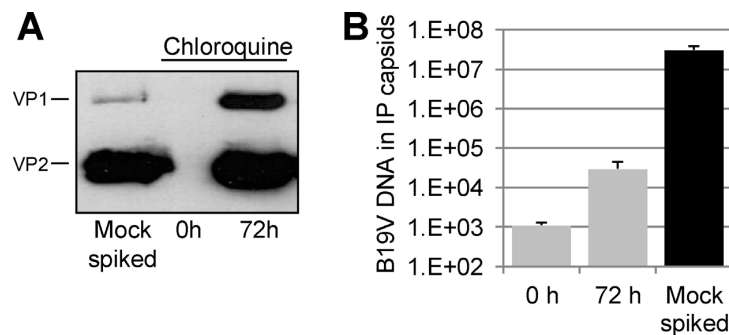
Fig. 4. Effect of chloroquine (CQ) in B19V infection in UT7/Epo cells. (A) Production of capsid progeny in UT7/Epo cells treated with CQ (25 μM). B19V capsids were immunoprecipitated from the cell extracts with mAb 860-55D. As a reference control, B19V (4×10^{10}) was added to mock-infected cell extracts. The production of capsid progeny in untreated UT7/Epo cells is shown in Fig. 1F. (B) B19V DNA was quantified from the immunoprecipitated capsids. As a reference control, B19V (4×10^{10} virions) was added to mock-infected cell extracts. Data are the mean ± SD for two independent experiments.
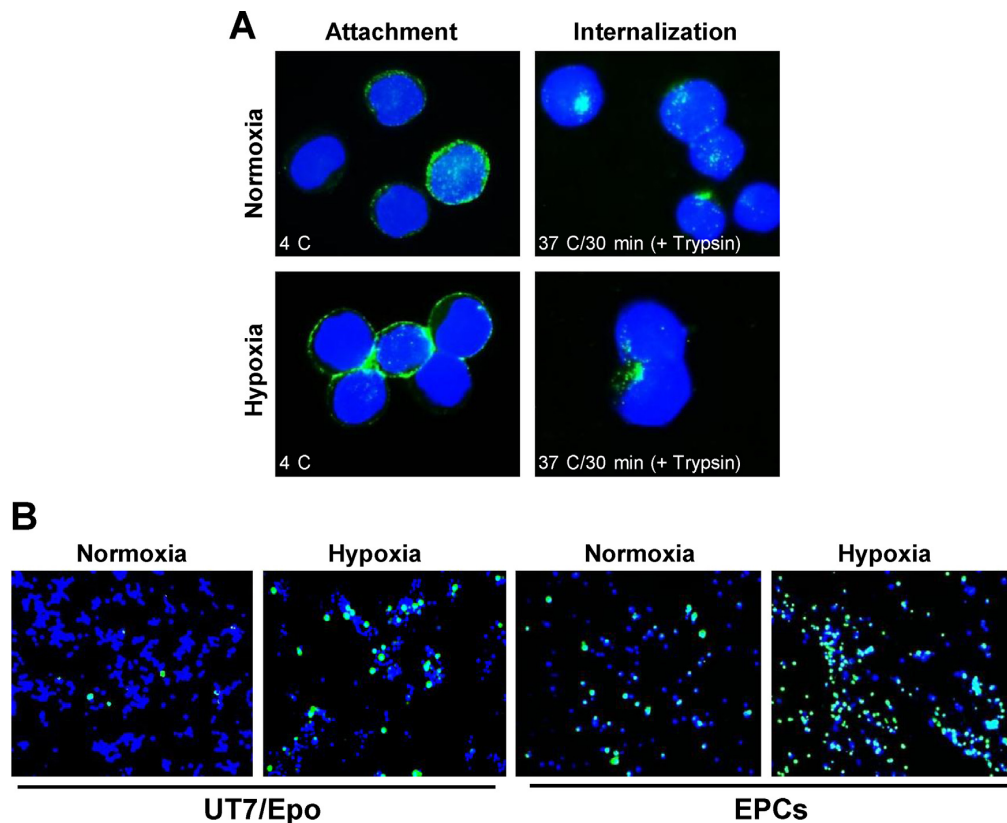
Fig. 5. Attachment, internalization and infection of B19V in EPCs under normoxia and hypoxia. Cells (3×10^5) were infected with B19V under normoxia or hypoxia. (A) Binding and internalization of B19V in EPCs. B19V was added to the cells at 4 °C for 1 h, washed, fixed and stained with an antibody against intact capsids. For internalization, the cells were further incubated for 30 min at 37 °C, washed and trypsinized to remove uninternalized particles. (B) Detection of virus progeny by IF 2 days p.i. in UT7/Epo cells and EPCs cultured under normoxic and hypoxic conditions.

3.7. VP1u conformation in the virus progeny differs from that of wild-type virus

The pores at the fivefold symmetry axis are the portals for the encapsidation of the viral genome but also for the externalization of VP1u. The fivefold cylinder is narrow and constrictions of the channel impair the encapsidation of the viral genome and the externalization of VP1u (Farr and Tattersall, 2004; Bleker et al., 2005, 2006; Plevka et al., 2011). Examination of the VP1u conformation in the mostly empty virus progeny revealed, that differently to the wild-type virus, VP1u was partially exposed. The most N-terminal part was accessible to antibodies, while the C-terminal region remained internal and inaccessible (Fig. 8B and C). Similar to other parvoviruses (Cotmore et al., 1999; Vihinen-Ranta et al., 2002), exposure to mild temperature triggers the externalization of the N-terminal and C-terminal regions of VP1u from B19V without capsid disassembly (Ros et al., 2006). In clear contrast to the wild-type virus, heat treatment did not trigger the externalization of the C-terminal region of VP1u from the capsid progeny generated under normoxia and only discretely from capsids generated under hypoxia (Fig. 8D). Therefore, the failure to encapsidate the viral genome is possibly due to the constriction of the fivefold axis channel by a partially exposed and inflexible VP1u.

4. Discussion

Discovered in 1975 (Cossart et al., 1975), today B19V is recognized as a major human pathogen involved in multiple syndromes.

However, the lack of a suitable cell culture system or an animal model restricts the availability of infectious virus and hampers seriously the studies with B19V. The virus has an extraordinary tropism for human erythroid progenitor cells (EPCs) in the bone marrow (Mortimer et al., 1983) where it can infect cells at the BFU-E and CFU-E stages of differentiation (Takahashi et al., 1990). During a natural infection B19V is able to replicate efficiently in the target cells, as judged by the typical high viremia observed in the infected individuals. However, the efficient B19V replication *in vivo* has not yet been mimicked *in vitro* with an established cell line, indicating the existence of highly restricted and still poorly understood cellular factors required for B19V replication. Some erythroleukemia cell lines, such as UT7/Epo (Shimomura et al., 1992) and KU812Ep6 (Miyagawa et al., 1999), have been shown to support B19V replication to a certain level, but none of them can produce significant quantities of infectious progeny. The human megakaryoblastic cell line UT7/Epo, has been shown to be the most permissive system for the *in vitro* replication of B19V (Wong and Brown, 2006) and it is used widely to study B19V infection.

The reason for the defective replication of B19V in these cells has been shown to be multifactorial. Restrictions occur already at the cell surface, by the variable and limited expression of receptors and co-receptors required for binding and internalization of B19V (Brown et al., 1993; Munakata et al., 2005; Weigel-Kelley et al., 2003), but also by required intracellular factors restricted mainly to the erythroid lineage. Those intracellular factors can operate at the level of transcription, controlling the generation of sufficient full-length capsid-encoding transcripts (Guan et al., 2008; Liu et al.,
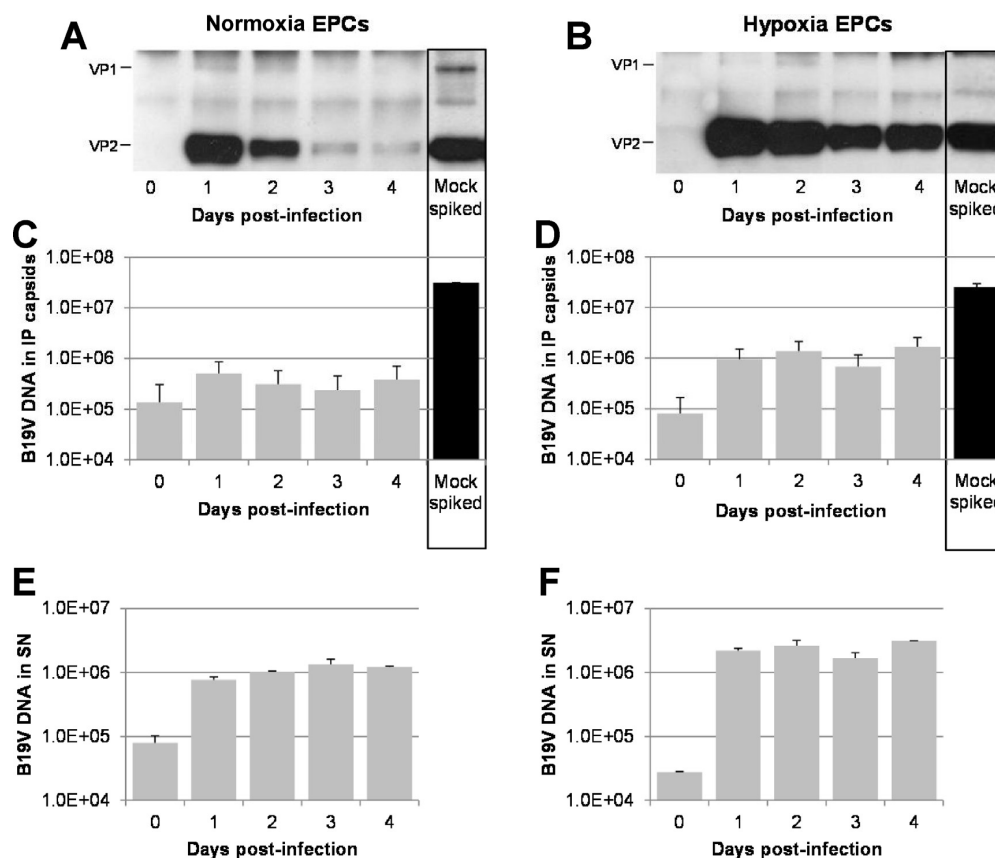
Fig. 6. Capsid progeny and quantitation of virions in EPCs. Cells (3×10^5) were infected with B19V under normoxia or hypoxia. At progressive times p.i., the supernatant was collected and the cells were lysed. (A and B) B19V capsids were immunoprecipitated from the cell extracts with mAb 860-55D, against intact capsids. As a reference control, B19V (4×10^{10}) was added to mock-infected cell extracts. (C and D) B19V DNA was quantified from the immunoprecipitated capsids. As a reference control, B19V (4×10^{10} virions) was added to mock-infected cell extracts. (E and F) B19V DNA was quantified from the supernatant of the infected cells. Data are the mean ± SD of two independent experiments.
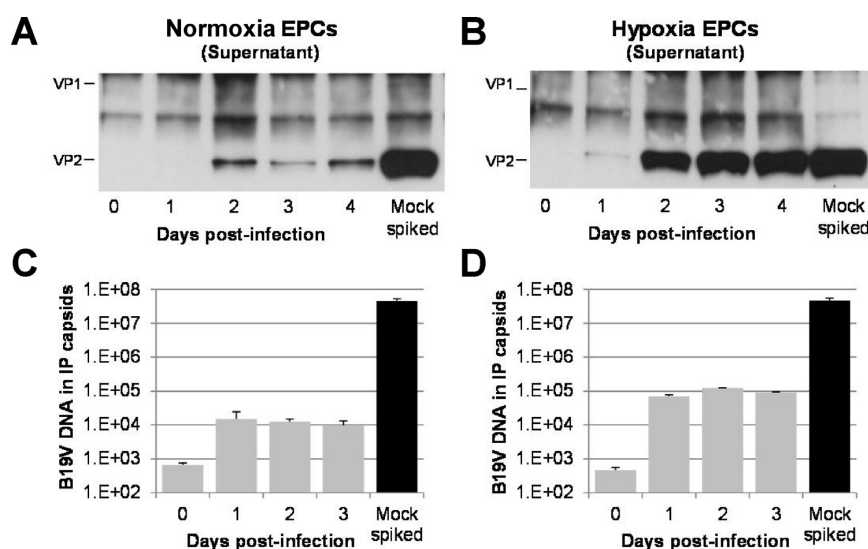

Fig. 7. Virus egress in EPCs. Cells (3×10^5) were infected with B19V under normoxia or hypoxia. (A and B) At progressive times p.i., B19V capsids were immunoprecipitated from the cell supernatant with mAb 860-55D. As a reference control, B19V (4×10^{10}) was added to mock-infected cell supernatant. (C and D) B19V capsids were immunoprecipitated and B19V DNA was quantified. As a reference control, B19V (4×10^{10} virions) was added to mock-infected cell supernatant. Data are the mean ± SD of two independent experiments.
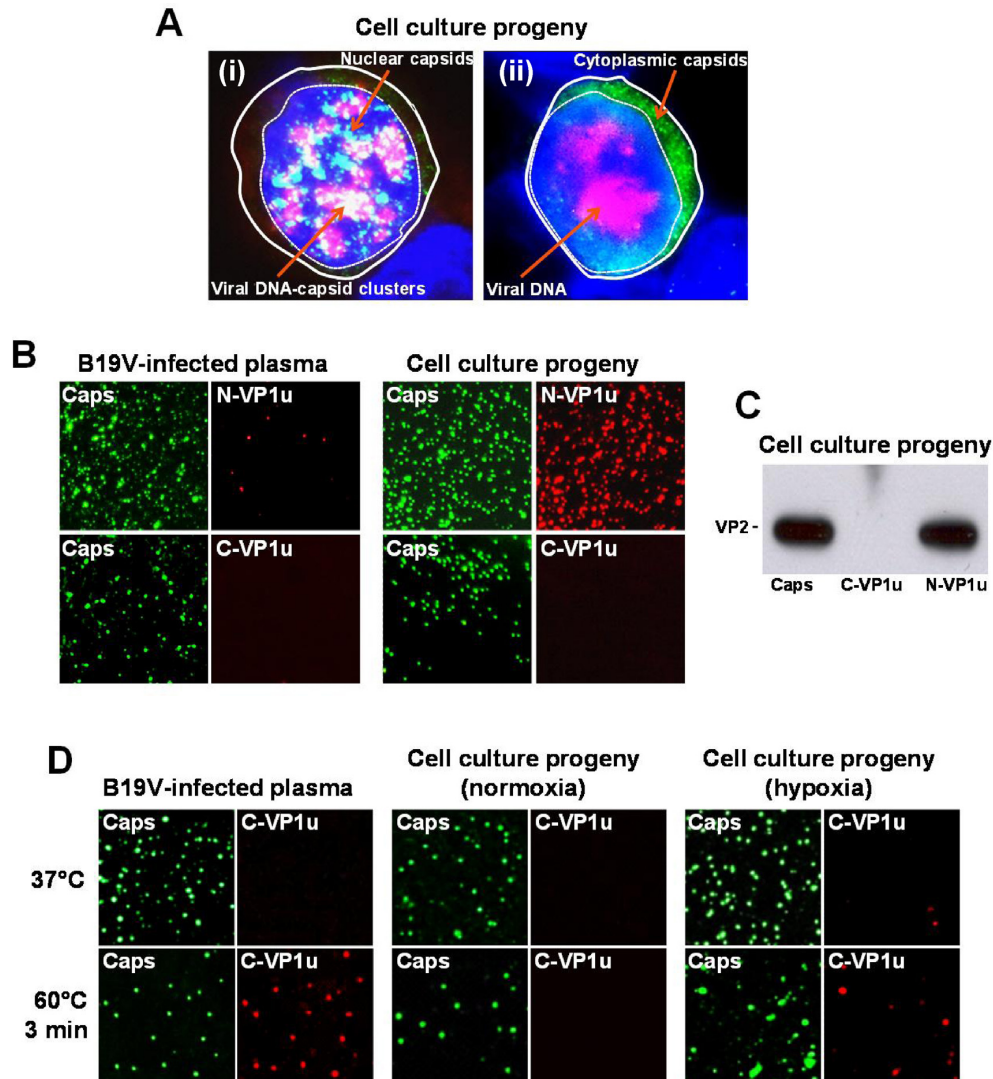
Fig. 8. Intracellular distribution of capsids and viral genomes and VP1u conformation in the capsid progeny. (A) Simultaneous detection of viral genomes and capsids in infected UT7Epo cells by FISH. Two representative cells are shown. (i) In some cells, B19V genomes and capsids were detectable in large clusters in the nucleus. (ii) In a larger proportion of cells, viral genomes were detected isolated in the nucleus while capsids were detected in the cytoplasm. (B) VP1u conformation in the plasma-derived virus differs from that of the cell culture progeny (UT7/Epo cells). Plasma-derived virus and cell culture progeny were concentrated by sucrose cushion centrifugation, spotted onto coverslips, fixed and detected by IF with mAb 860-55D or mAb 521-5D (Caps) and antibodies against the N-terminal and C-terminal regions of VP1u. (C) Immunoprecipitation of the cell culture progeny (UT7/Epo cells, 3 days p.i.) with mAb 860-55D (Capsids) and antibodies against the N-terminus and C-terminus of VP1u. (D) Flexibility of VP1u in the plasma-derived virus and cell culture progeny obtained under normoxia or hypoxia. Viruses were untreated (37 °C) or heat-treated (60 °C for 3 min) to trigger the exposure of VP1u and detected by IF with the indicated antibodies.

1992). In non-permissive cells the majority of viral mRNAs encode for NS1, with only limited production of the capsid-encoding transcripts. NS1 causes cell death by its cytotoxic or apoptotic characteristics (Moffatt et al., 1998). In contrast, more B19V RNAs are read through the multiple polyadenylation sites in permissive cells, which results in sufficient full-length capsid-encoding mRNAs (Liu et al., 1992). Studies have also shown that B19V replication and transcription were restricted to a small subset of cells but without production of capsid proteins, while in other cells, the single-stranded viral DNA was not converted to the double-stranded form (Gallinella et al., 2000). All the described restrictions at early (receptor/co-receptor) and late (replication/transcription) stages of the infection result in none or limited production of virus progeny.

Recently, two novel approaches based on hypoxic conditions (Caillet-Fauquet et al., 2004b; Pillet et al., 2004) and the use of *ex vivo* expanded CD36+ primary human erythroid progenitor cells (CD36+ EPCs), previous CD34+ *in vitro* preselection (Pillet et al., 2008; Wong et al., 2008), or directly from unselected peripheral blood mononuclear cells (Filippone et al., 2010), have been shown to improve B19V infection. The obtained results are in agreement with previous observations, which showed that B19V replicates better in CD36+ EPCs, in particular under hypoxia (Chen et al., 2011). However, despite these improvements, the final genome encapsidation step was still insufficient, producing abundant but mostly non-infectious empty capsids. In the study by Chen et al. (2011), the use of EPCs under hypoxia was shown to improve B19V infection, however large quantities of infectious virus were not

recovered from the supernatant of the infected cells, as it should be expected for a lytic virus. Therefore, CD36+ EPCs cannot yet be considered as a highly permissive cell culture system to propagate B19V and a robust source of infectious virus. Moreover, compared to UT7/Epo cells, the generation of primary CD36+ EPCs remains time-consuming, requires large quantities of expensive growth factors and the permissivity to B19V is limited within a narrow and variable time-frame when B19V receptor and co-receptors are expressed in concert with a favorable intracellular microenvironment (Wong et al., 2008).

Parvoviruses pack their single-stranded, linear DNA genome into the pre-assembled capsids in the nucleus (Cotmore and Tattersall, 2005; King et al., 2001; Timpe et al., 2005). The helicase activity of the parvovirus nonstructural protein, which is present in the encapsidation complexes, functions as a molecular motor to translocate the viral genome into the empty capsid through the fivefold axes pore, a process that is also mediated by the terminal telomeric structures of the viral genome (Cotmore and Tattersall, 2005; King et al., 2001). Besides genome encapsidation, the channels at the fivefold symmetry axis are also used for the externalization of VP1u during the infection process (Bleker et al., 2005, 2006; Cotmore and Tattersall, 2012; Farr and Tattersall, 2004; Plevka et al., 2011). The channel is narrow and minor modifications of its diameter result in defective genome encapsidation and VP1u externalization (Bleker et al., 2005; Cotmore and Tattersall, 2012). Therefore, specific capsid and genome conformations play a critical role in the packaging step. VP1u from parvoviruses is not accessible, but can become exposed *in vitro* by mild heat or low pH treatments and *in vivo* during the intracellular trafficking of the virus (Cotmore et al., 1999; Kronenberg et al., 2005; Mani et al., 2006; Ros et al., 2006; Vihinen-Ranta et al., 2002) or upon receptor binding in the case of B19V (Bönsch et al., 2010a). In clear contrast to natural plasma-derived virus, VP1u was exposed partially in the capsid progeny. While the most N-terminal region was externalized and accessible to antibodies, the C-terminal region remained internal (Fig. 8). This particular conformation was irreversible and did not change upon heat treatment. The aberrant conformation and rigidity of VP1u might explain the encapsidation failure in semi-permissive cell systems. Further studies will elucidate whether the VP1u conformation in the virus progeny is due to an aberrant assembly or the lack of a final maturation step.

5. Conclusions

When compared to UT7/Epo cells and normoxia, hypoxic conditions or the use of CD36+ EPCs resulted in a significant acceleration of the infection/transfection, an increase in the number of infected cells and a modest increase in the yield of capsid progeny. However, despite these improvements, genome encapsidation was impaired seriously under all tested conditions and cells. The fivefold axes channel might be constricted in the virus progeny by the atypical partial exposure of VP1u hindering the packaging step, which arises as a major limiting factor for the *in vitro* propagation of B19V.

Acknowledgments

References

Bleker, S., Pawlita, M., Kleinschmidt, J.A., 2006. Impact of capsid conformation and Rep-capsid interactions on adeno-associated virus type 2 genome packaging. J. Virol. 80, 810–820.
Bleker, S., Sonntag, F., Kleinschmidt, J.A., 2005. Mutational analysis of narrow pores at the fivefold symmetry axes of adeno-associated virus type 2 capsids reveals a dual role in genome packaging and activation of phospholipase A2 activity. J. Virol. 79, 2528–2540.
Bönsch, C., Zuercher, C., Lieby, P., Kempf, C., Ros, C., 2010a. The globoside receptor triggers structural changes in the B19 virus capsid that facilitate virus internalization. J. Virol. 84, 11737–11746.
Bönsch, C., Kempf, C., Mueller, I., Manning, L., Laman, M., Davis, T.M., Ros, C., 2010b. Chloroquine and its derivatives exacerbate B19V-associated anemia by promoting viral replication. PLoS Negl. Trop. Dis. 4 (4), e669.
Bönsch, C., Kempf, C., Ros, C., 2008. Interaction of parvovirus B19 with human erythrocytes alters virus structure and cell membrane integrity. J. Virol. 82, 11784–11791.
Bonvicini, F., Filippone, C., Manaresi, E., Zerbini, M., Musiani, M., Gallinella, G., 2008. HepG2 hepatocellular carcinoma cells are a non-permissive system for B19 virus infection. J. Gen. Virol. 89, 3034–3038.
Brown, K.E., Anderson, S.M., Young, N.S., 1993. Erythrocyte P antigen: cellular receptor for B19 parvovirus. Science 262, 114–117.
Brunstein, J., Söderlund-Venermo, M., Hedman, K., 2000. Identification of a novel RNA splicing pattern as a basis of restricted cell tropism of erythrovirus B19. Virology 274, 284–291.
Caillet-Fauquet, P., Di Giambattista, M., Draps, M.L., Hougardy, V., de Launoit, Y., Laub, R., 2004a. An assay for parvovirus B19 neutralizing antibodies based on human hepatocarcinoma cell lines. Transfusion 44, 1340–1343.
Caillet-Fauquet, P., Draps, M.L., Di Giambattista, M., de Launoit, Y., Laub, R., 2004b. Hypoxia enables B19 erythrovirus to yield abundant infectious progeny in a pluripotent erythroid cell line. J. Virol. Methods 121, 145–153.
Chen, A.Y., Kleiboeker, S., Qiu, J., 2011. Productive parvovirus B19 infection of primary human erythroid progenitor cells at hypoxia is regulated by STAT5A and MEK signaling but not HIFα. PLoS Pathog. 7 (6), e1002088.
Chen, A.Y., Guan, W., Lou, S., Liu, Z., Kleiboeker, S., Qiu, J., 2010. Role of erythropoietin receptor signaling in parvovirus B19 replication in human erythroid progenitor cells. J. Virol. 84, 12385–12396.
Cossart, Y.E., Field, A.M., Cant, B., Widdows, D., 1975. Parvovirus-like particles in human sera. Lancet 1, 72–73.
Cotmore, S.F., Tattersall, P., 2012. Mutations at the base of the icosahedral five-fold cylinders of minute virus of mice induce 3′-to-5′ genome uncoating and critically impair entry functions. J. Virol. 86, 69–80.
Cotmore, S.F., Tattersall, P., 2005. Encapsidation of minute virus of mice DNA: aspects of the translocation mechanism revealed by the structure of partially packaged genomes. Virology 336, 100–112.
Cotmore, S.F., D'abramo Jr., A.M., Ticknor, C.M., Tattersall, P., 1999. Controlled conformational transitions in the MVM virion expose the VP1 N-terminus and viral genome without particle disassembly. Virology 254, 169–181.
Farr, G.A., Tattersall, P., 2004. A conserved leucine that constricts the pore through the capsid fivefold cylinder plays a central role in parvoviral infection. Virology 323, 243–256.
Filippone, C., Franssila, R., Kumar, A., Saikko, L., Kovanen, P.E., Söderlund-Venermo, M., Hedman, K., 2010. Erythroid progenitor cells expanded from peripheral blood without mobilization or preselection: molecular characteristics and functional competence. PLoS One 5 (3), e9496.
Gallinella, G., Manaresi, E., Zuffi, E., Venturoli, S., Bonsi, L., Bagnara, G.P., Musiani, M., Zerbini, M., 2000. Different patterns of restriction to B19 parvovirus replication in human blast cell lines. Virology 278, 361–367.
Gigler, A., Dorsch, S., Hemauer, A., Williams, C., Kim, S., Young, N.S., Zolla-Pazner, S., Wolf, H., Gorny, M.K., Modrow, S., 1999. Generation of neutralizing human monoclonal antibodies against parvovirus B19 proteins. J. Virol. 73, 1974–1979.
Guan, W., Cheng, F., Yoto, Y., Kleiboeker, S., Wong, S., Zhi, N., Pintel, D.J., Qiu, J., 2008. Block to the production of full-length B19 virus transcripts by internal polyadenylation is overcome by replication of the viral genome. J. Virol. 82, 9951–9963.
Heegaard, E.D., Brown, K.E., 2002. Human parvovirus B19. Clin. Microbiol. Rev. 15, 485–505.
Heegaard, E.D., Hornsleth, A., 1995. Parvovirus: the expanding spectrum of disease. Acta Paediatr. 84, 109–117.
Hunter, L.A., Samulski, R.J., 1992. Colocalization of adeno-associated virus Rep and capsid proteins in the nuclei of infected cells. J. Virol. 66, 317–324.
King, J.A., Dubielzig, R., Grimm, D., Kleinschmidt, J.A., 2001. DNA helicase-mediated packaging of adeno-associated virus type 2 genomes into preformed capsids. EMBO J. 20, 3282–3291.
Kooistra, K., Mesman, H.J., de Waal, M., Koppelman, M.H., Zaaijer, H.L., 2011. Epidemiology of high-level parvovirus B19 viraemia among Dutch blood donors, 2003–2009. Vox Sang. 100, 261–266.
Kronenberg, S., Bottcher, B., von der Lieth, C.W., Bleker, S., Kleinschmidt, J.A., 2005. A conformational change in the adeno-associated virus type 2 capsid leads to the exposure of hidden VP1N termini. J. Virol. 79, 5296–5303.
Liu, J.M., Green, S.W., Shimada, T., Young, N.S., 1992. A block in full-length transcript maturation in cells nonpermissive for B19 parvovirus. J. Virol. 66, 4686–4692.

Luo, Y., Lou, S., Deng, X., Liu, Z., Li, Y., Kleiboeker, S., Qiu, J., 2011. Parvovirus B19 infection of human primary erythroid progenitor cells triggers ATR-Chk1 signaling, which promotes B19 virus replication. J. Virol. 85, 8046–8055.

Mani, B., Baltzer, C., Valle, N., Almendral, J.M., Kempf, C., Ros, C., 2006. Low pH-dependent endosomal processing of the incoming parvovirus minute virus of mice virion leads to externalization of the VP1 N-terminal sequence (N-VP1), N-VP2 cleavage, and uncoating of the full-length genome. J. Virol. 80, 1015–1024.

Miyagawa, E., Yoshida, T., Takahashi, H., Yamaguchi, K., Nagano, T., Kiriyama, Y., Okochi, K., Sato, H., 1999. Infection of the erythroid cell line, KU812Ep6 with human parvovirus B19 and its application to titration of B19 infectivity. J. Virol. Methods 83, 45–54.

Moffatt, S., Yaegashi, N., Tada, K., Tanaka, N., Sugamura, K., 1998. Human parvovirus B19 nonstructural (NS1) protein induces apoptosis in erythroid lineage cells. J. Virol. 72, 3018–3028.

Mortimer, P.P., Humphries, R.K., Moore, J.G., Purcell, R.H., Young, N.S., 1983. A human parvovirus-like virus inhibits haematopoietic colony formation in vitro. Nature 302, 426–429.

Munakata, Y., Saito-Ito, T., Kumura-Ishii, K., Huang, J., Kodera, T., Ishii, T., Hirabayashi, Y., Koyanagi, Y., Sasaki, T., 2005. Ku80 autoantigen as a cellular coreceptor for human parvovirus B19 infection. Blood 106, 3449–3456.

Ozawa, K., Kurtzman, G., Young, N., 1987. Productive infection by B19 parvovirus of human erythroid bone marrow cells in vitro. Blood 70, 384–391.

Ozawa, K., Kurtzman, G., Young, N., 1986. Replication of the B19 parvovirus in human bone marrow cell cultures. Science 233, 883–886.

Pallier, C., Greco, A., Le Junter, J., Saib, A., Vassias, I., Morinet, F., 1997. The 3′ untranslated region of the B19 parvovirus capsid protein mRNAs inhibits its own mRNA translation in nonpermissive cells. J. Virol. 71, 9482–9489.

Pillet, S., Fichelson, S., Morinet, F., Young, N.S., Zhi, N., Wong, S., 2008. Human B19 erythrovirus in vitro replication: what's new? J. Virol. 82, 8951–8953.

Pillet, S., Le Guyader, N., Hofer, T., NguyenKhac, F., Koken, M., Aubin, J.T., Fichelson, S., Gassmann, M., Morinet, F., 2004. Hypoxia enhances human B19 erythrovirus gene expression in primary erythroid cells. Virology 327, 1–7.

Plevka, P., Hafenstein, S., Li, L., D'Abrgamo Jr., A., Cotmore, S.F., Rossmann, M.G., Tattersall, P., 2011. Structure of a packaging-defective mutant of minute virus of mice indicates that the genome is packaged via a pore at a 5-fold axis. J. Virol. 85, 4822–4827.

Ros, C., Gerber, M., Kempf, C., 2006. Conformational changes in the VP1-unique region of native human parvovirus B19 lead to exposure of internal sequences that play a role in virus neutralization and infectivity. J. Virol. 80, 12017–12024.

Servey, J.T., Reamy, B.V., Hodge, J., 2007. Clinical presentations of parvovirus B19 infection. Am. Fam. Physician 75, 373–376.

Shimomura, S., Komatsu, N., Frickhofen, N., Anderson, S., Kajigaya, S., Young, N.S., 1992. First continuous propagation of B19 parvovirus in a cell line. Blood 79, 18–24.

Takahashi, T., Ozawa, K., Takahashi, K., Asano, S., Takaku, F., 1990. Susceptibility of human erythropoietic cells to B19 parvovirus in vitro increases with differentiation. Blood 75, 603–610.

Timpe, J., Bevington, J., Casper, J., Dignam, J.D., Trempe, J.P., 2005. Mechanisms of adeno-associated virus genome encapsidation. Curr. Gene Ther. 5, 273–284.

Vihinen-Ranta, M., Wang, D., Weichert, W.S., Parrish, C.R., 2002. The VP1 N-terminal sequence of canine parvovirus affects nuclear transport of capsids and efficient cell infection. J. Virol. 76, 1884–1891.

Weigel-Kelley, K.A., Yoder, M.C., Srivastava, A., 2003. Alpha5beta1 integrin as a cellular coreceptor for human parvovirus B19: requirement of functional activation of beta1 integrin for viral entry. Blood 102, 3927–3933.

Wistuba, A., Kern, A., Weger, S., Grimm, D., Kleinschmidt, J.A., 1997. Subcellular compartmentalization of adeno-associated virus type 2 assembly. J. Virol. 71, 1341–1352.

Wong, S., Zhi, N., Filippone, C., Keyvanfar, K., Kajigaya, S., Brown, K.E., Young, N.S., 2008. Ex vivo-generated CD36+ erythroid progenitors are highly permissive to human parvovirus B19 replication. J. Virol. 82, 2470–2476.

Wong, S., Brown, K.E., 2006. Development of an improved method of detection of infectious parvovirus B19. J. Clin. Virol. 35, 407–413.

Zhi, N., Zádori, Z., Brown, K.E., Tijssen, P., 2004. Construction and sequencing of an infectious clone of the human parvovirus B19. Virology 318, 142–152.

Part III

Discussion

Bibliography

[1] R. SAHLI, G. K. MCMASTER, and B. HIRT, DNA sequence comparison between two tissue-specific variants of the autonomous parvovirus, minute virus of mice, *Nucleic Acids Res.* **13**, 3617 (1985).

[2] L. V. CRAWFORD, A minute virus of mice, *Virology* **29**, 605 (1966).

[3] P. TATTERSALL, Replication of the parvovirus MVM. I. Dependence of virus multiplication and plaque formation on cell growth, *J. Virol.* **10**, 586 (1972).

[4] B. A. SPALHOLZ, J. BRATTON, D. C. WARD, and P. TATTERSALL, *Tumor Viruses and Differentiation*, Academic Press, New York, NY, 1982.

[5] G. D. BONNARD, E. K. MANDERS, D. A. CAMPBELL, R. B. HERBERMAN, and M. J. COLLINS, Immunosuppressive activity of a subline of the mouse EL-4 lymphoma. Evidence for minute virus of mice causing the inhibition, *J. Exp. Med.* **143**, 187 (1976).

[6] H. D. ENGERS, J. A. LOUIS, R. H. ZUBLER, and B. HIRT, Inhibition of T cell-mediated functions by MVM(i), a parvovirus closely related to minute virus of mice, *J. Immunol.* **127**, 2280 (1981).

[7] G. K. MCMASTER, P. BEARD, H. D. ENGERS, and B. HIRT, Characterization of an immunosuppressive parvovirus related to the minute virus of mice, *J. Virol.* **38**, 317 (1981).

[8] L. V. CRAWFORD, E. A. FOLLETT, M. G. BURDON, and D. J. MCGEOCH, The DNA of a minute virus of mice, *J. Gen. Virol.* **4**, 37 (1969).

[9] J. A. ROSE, K. I. BERNS, M. D. HOGGAN, and F. J. KOCZOT, Evidence for a single-stranded adenovirus-associated virus genome: formation of a DNA density hybrid on release of viral DNA, *Proc. Natl. Acad. Sci. U.S.A.* **64**, 863 (1969).

[10] K. I. BERNS and J. A. ROSE, Evidence for a single-stranded adenovirus-associated virus genome: isolation and separation of complementary single strands, *J. Virol.* **5**, 693 (1970).

[11] P. TIJSSEN, Molecular and structural basis of the evolution of parvovirus tropism, *Acta Vet. Hung.* **47**, 379 (1999).

[12] A. M. Q. KING, M. J. ADAMS, E. B. CARSTENS, and E. J. LEFKOWITZ, *Virus taxonomy: Ninth report of the International Committee on Taxonomy of Viruses.*, Elsevier Academic Press, San Diego, CA, 2012.

[13] M. D. HOGGAN, K. MARAMOROSCH, and E. KURSTAK, *Small DNA viruses*, Academic Press, New York, NY, 1971.

[14] L. A. SALZMAN and L. A. JORI, Characterization of the Kilham rat virus, *J. Virol.* **5**, 114 (1970).

[15] N. BOSCHETTI, K. WYSS, A. MISCHLER, T. HOSTETTLER, and C. KEMPF, Stability of minute virus of mice against temperature and sodium hydroxide, *Biologicals* **31**, 181 (2003).

[16] J. BLUMEL, I. SCHMIDT, H. WILLKOMMEN, and J. LOWER, Inactivation of parvovirus B19 during pasteurization of human serum albumin, *Transfusion* **42**, 1011 (2002).

[17] B. MANI, M. GERBER, P. LIEBY, N. BOSCHETTI, C. KEMPF, and C. ROS, Molecular mechanism underlying B19 virus inactivation and comparison to other parvoviruses, *Transfusion* **47**, 1765 (2007).

[18] A. SAUERBREI and P. WUTZLER, Testing thermal resistance of viruses, *Arch. Virol.* **154**, 115 (2009).

[19] R. E. HARRIS, P. H. COLEMAN, and P. S. MORAHAN, Stability of minute virus of mice to chemical and physical agents, *Appl Microbiol* **28**, 351 (1974).

[20] M. SAKNIMIT, I. INATSUKI, Y. SUGIYAMA, and K. YAGAMI, Virucidal efficacy of physico-chemical treatments against coronaviruses and parvoviruses of laboratory animals, *Jikken Dobutsu* **37**, 341 (1988).

[21] S. BRAUNIGER, I. FISCHER, and J. PETERS, [The temperature stability of bovine parvovirus], *Zentralbl Hyg Umweltmed* **196**, 270 (1994).

[22] T. F. SCHWARZ, S. SERKE, A. VON BRUNN, B. HOTTENTRAGER, D. HUHN, F. DEINHARDT, and M. ROGGENDORF, Heat stability of parvovirus B19: kinetics of inactivation, *Zentralbl. Bakteriol.* **277**, 219 (1992).

[23] C. BRAILOVSKY, [Research on the rat K virus (Parvovirus ratti). I. A method of titration by plaques and its application to the study of the multiplication cycle of the virus], *Ann Inst Pasteur (Paris)* **110**, 49 (1966).

[24] V. A. BELYI, A. J. LEVINE, and A. M. SKALKA, Sequences from ancestral single-stranded DNA viruses in vertebrate genomes: the parvoviridae and circoviridae are more than 40 to 50 million years old, *J. Virol.* **84**, 12458 (2010).

[25] E. GOTTSCHALCK, S. ALEXANDERSEN, A. COHN, L. A. POULSEN, M. E. BLOOM, and B. AASTED, Nucleotide sequence analysis of Aleutian mink disease parvovirus shows that multiple virus types are present in infected mink, *J. Virol.* **65**, 4378 (1991).

[26] G. GAO, M. R. ALVIRA, S. SOMANATHAN, Y. LU, L. H. VANDENBERGHE, J. J. RUX, R. CALCEDO, J. SANMIGUEL, Z. ABBAS, and J. M. WILSON, Adeno-associated viruses undergo substantial evolution in primates during natural infections, *Proc. Natl. Acad. Sci. U.S.A.* **100**, 6081 (2003).

[27] H. A. WICHMAN, M. R. BADGETT, L. A. SCOTT, C. M. BOULIANNE, and J. J. BULL, Different trajectories of parallel evolution during viral adaptation, *Science* **285**, 422 (1999).

[28] L. A. SHACKELTON and E. C. HOLMES, Phylogenetic evidence for the rapid evolution of human B19 erythrovirus, *J. Virol.* **80**, 3666 (2006).

[29] L. A. SHACKELTON, C. R. PARRISH, U. TRUYEN, and E. C. HOLMES, High rate of viral evolution associated with the emergence of carnivore parvovirus, *Proc. Natl. Acad. Sci. U.S.A.* **102**, 379 (2005).

[30] A. F. STRECK, S. L. BONATTO, T. HOMEIER, C. K. SOUZA, K. R. GONCALVES, D. GAVA, C. W. CANAL, and U. TRUYEN, High rate of viral evolution in the capsid protein of porcine parvovirus, *J. Gen. Virol.* **92**, 2628 (2011).

[31] M. LEDERMAN, J. T. PATTON, E. R. STOUT, and R. C. BATES, Virally coded noncapsid protein associated with bovine parvovirus infection, *J. Virol.* **49**, 315 (1984).

[32] W. X. CHENG, J. S. LI, C. P. HUANG, D. P. YAO, N. LIU, S. X. CUI, Y. JIN, and Z. J. DUAN, Identification and nearly full-length genome characterization of novel porcine bocaviruses, *PLoS ONE* **5**, e13583 (2010).

[33] A. K. Cheung, G. Wu, D. Wang, D. O. Bayles, K. M. Lager, and A. L. Vincent, Identification and molecular cloning of a novel porcine parvovirus, *Arch. Virol.* **155**, 801 (2010).

[34] S. F. Cotmore and P. Tattersall, The autonomously replicating parvoviruses of vertebrates, *Adv. Virus Res.* **33**, 91 (1987).

[35] S. F. Cotmore, M. Agbandje-McKenna, J. A. Chiorini, D. V. Mukha, D. J. Pintel, J. Qiu, M. Soderlund-Venermo, P. Tattersall, P. Tijssen, D. Gatherer, and A. J. Davison, The family Parvoviridae, *Arch. Virol.* **159**, 1239 (2014).

[36] V. V. Lukashov and J. Goudsmit, Evolutionary relationships among parvoviruses: virus-host coevolution among autonomous primate parvoviruses and links between adeno-associated and avian parvoviruses, *J. Virol.* **75**, 2729 (2001).

[37] M. E. Bloom, R. E. Race, and J. B. Wolfinbarger, Characterization of Aleutian disease virus as a parvovirus, *J. Virol.* **35**, 836 (1980).

[38] S. Alexandersen, M. E. Bloom, and S. Perryman, Detailed transcription map of Aleutian mink disease parvovirus, *J. Virol.* **62**, 3684 (1988).

[39] J. Qiu, F. Cheng, L. R. Burger, and D. Pintel, The transcription profile of Aleutian mink disease virus in CRFK cells is generated by alternative processing of pre-mRNAs produced from a single promoter, *J. Virol.* **80**, 654 (2006).

[40] L. Li, P. A. Pesavento, L. Woods, D. L. Clifford, J. Luff, C. Wang, and E. Delwart, Novel amdovirus in gray foxes, *Emerging Infect. Dis.* **17**, 1876 (2011).

[41] R. McKenna, N. H. Olson, P. R. Chipman, T. S. Baker, T. F. Booth, J. Christensen, B. Aasted, J. M. Fox, M. E. Bloom, J. B. Wolfinbarger, and M. Agbandje-McKenna, Three-dimensional structure of Aleutian mink disease parvovirus: implications for disease pathogenicity, *J. Virol.* **73**, 6882 (1999).

[42] J. Kisary, B. Nagy, and Z. Bitay, Presence of parvoviruses in the intestine of chickens showing stunting syndrome, *Avian Pathol.* **13**, 339 (1984).

[43] D. W. Trampel, D. A. Kinden, R. F. Solorzano, and P. L. Stogsdill, Parvovirus-like enteropathy in Missouri turkeys, *Avian Dis.* **27**, 49 (1983).

[44] J. Kisary, B. Avalosse, A. Miller-Faures, and J. Rommelaere, The genome structure of a new chicken virus identifies it as a parvovirus, *J. Gen. Virol.* **66 (Pt 10)**, 2259 (1985).

[45] B. S. Koo, H. R. Lee, E. O. Jeon, M. S. Han, K. C. Min, S. B. Lee, Y. J. Bae, S. H. Cho, J. S. Mo, H. M. Kwon, H. W. Sung, J. N. Kim, and I. P. Mo, Genetic characterization of three novel chicken parvovirus strains based on analysis of their coding sequences, *Avian Pathol.* **44**, 28 (2015).

[46] L. Zsak, K. O. Strother, and J. Kisary, Partial genome sequence analysis of parvoviruses associated with enteric disease in poultry, *Avian Pathol.* **37**, 435 (2008).

[47] J. M. Day and L. Zsak, Determination and analysis of the full-length chicken parvovirus genome, *Virology* **399**, 59 (2010).

[48] J. Kisary, Experimental infection of chicken embryos and day-old chickens with parvovirus of chicken origin, *Avian Pathol.* **14**, 1 (1985).

[49] R. K. Page, O. J. Fletcher, G. N. Rowland, D. Gaudry, and P. Villegas, Malabsorption syndrome in broiler chickens, *Avian Dis.* **26**, 618 (1982).

[50] D. A. Pass, M. D. Robertson, and G. E. Wilcox, Runting syndrome in broiler chickens in Australia, *Vet. Rec.* **110**, 386 (1982).

[51] M. A. Goodwin, J. F. Davis, M. S. McNulty, J. Brown, and E. C. Player, Enteritis (so-called runting stunting syndrome) in Georgia broiler chicks, *Avian Dis.* **37**, 451 (1993).

[52] H. J. Barnes, J. S. Guy, and J. P. Vaillancourt, Poult enteritis complex, *Rev. - Off. Int. Epizoot.* **19**, 565 (2000).

[53] Y. M. Saif, H. J. Barnes, J. R. Glisson, A. M. Fadly, L. R. McDougald, and D. E. Swayne, *Diseases of Poultry 11th edn*, Wiley-Blackwell, Hoboken, NJ, 2003, pp 1171-1180.

[54] K. C. Chen, B. C. Shull, E. A. Moses, M. Lederman, E. R. Stout, and R. C. Bates, Complete nucleotide sequence and genome organization of bovine parvovirus, *J. Virol.* **60**, 1085 (1986).

[55] D. Schwartz, B. Green, L. E. Carmichael, and C. R. Parrish, The canine minute virus (minute virus of canines) is a distinct parvovirus that is most similar to bovine parvovirus, *Virology* **302**, 219 (2002).

[56] J. Qiu, F. Cheng, F. B. Johnson, and D. Pintel, The transcription profile of the bocavirus bovine parvovirus is unlike those of previously characterized parvoviruses, *J. Virol.* **81**, 12080 (2007).

[57] T. ALLANDER, S. U. EMERSON, R. E. ENGLE, R. H. PURCELL, and J. BUKH, A virus discovery method incorporating DNase treatment and its application to the identification of two bovine parvovirus species, *Proc. Natl. Acad. Sci. U.S.A.* **98**, 11609 (2001).

[58] T. ALLANDER, M. T. TAMMI, M. ERIKSSON, A. BJERKNER, A. TIVELJUNG-LINDELL, and B. ANDERSSON, Cloning of a human parvovirus by molecular screening of respiratory tract samples, *Proc. Natl. Acad. Sci. U.S.A.* **102**, 12891 (2005).

[59] D. VICENTE, G. CILLA, M. MONTES, E. G. PEREZ-YARZA, and E. PEREZ-TRALLERO, Human bocavirus, a respiratory and enteric virus, *Emerging Infect. Dis.* **13**, 636 (2007).

[60] N. BASTIEN, N. CHUI, J. L. ROBINSON, B. E. LEE, K. DUST, L. HART, and Y. LI, Detection of human bocavirus in Canadian children in a 1-year study, *J. Clin. Microbiol.* **45**, 610 (2007).

[61] X. MA, R. ENDO, N. ISHIGURO, T. EBIHARA, H. ISHIKO, T. ARIGA, and H. KIKUTA, Detection of human bocavirus in Japanese children with lower respiratory tract infections, *J. Clin. Microbiol.* **44**, 1132 (2006).

[62] A. MANNING, V. RUSSELL, K. EASTICK, G. H. LEADBETTER, N. HALLAM, K. TEMPLETON, and P. SIMMONDS, Epidemiological profile and clinical associations of human bocavirus and other human parvoviruses, *J. Infect. Dis.* **194**, 1283 (2006).

[63] B. KUPFER, J. VEHRESCHILD, O. CORNELY, R. KAISER, G. PLUM, S. VIAZOV, C. FRANZEN, R. L. TILLMANN, A. SIMON, A. MULLER, and O. SCHILDGEN, Severe pneumonia and human bocavirus in adult, *Emerging Infect. Dis.* **12**, 1614 (2006).

[64] L. HUANG, S. L. ZHAI, A. K. CHEUNG, H. B. ZHANG, J. X. LONG, and S. S. YUAN, Detection of a novel porcine parvovirus, PPV4, in Chinese swine herds, *Virol. J.* **7**, 333 (2010).

[65] A. L. BLOMSTROM, K. STAHL, C. MASEMBE, E. OKOTH, A. R. OKURUT, P. ATMNEDI, S. KEMP, R. BISHOP, S. BELAK, and M. BERG, Viral metagenomic analysis of bushpigs (Potamochoerus larvatus) in Uganda identifies novel variants of Porcine parvovirus 4 and Torque teno sus virus 1 and 2, *Virol. J.* **9**, 192 (2012).

[66] C. T. Xiao, P. G. Halbur, and T. Opriessnig, Complete Genome Sequence of a Novel Porcine Parvovirus (PPV) Provisionally Designated PPV5, *Genome Announc* **1** (2013).

[67] J. Ni, C. Qiao, X. Han, T. Han, W. Kang, Z. Zi, Z. Cao, X. Zhai, and X. Cai, Identification and genomic characterization of a novel porcine parvovirus (PPV6) in china, *Virol. J.* **11**, 203 (2014).

[68] C. T. Xiao, L. G. Gimenez-Lirola, Y. H. Jiang, P. G. Halbur, and T. Opriessnig, Characterization of a novel porcine parvovirus tentatively designated PPV5, *PLoS ONE* **8**, e65312 (2013).

[69] L. A. van Leengoed, J. Vos, E. Gruys, P. Rondhuis, and A. Brand, Porcine Parvovirus infection: review and diagnosis in a sow herd with reproductive failure, *Vet Q* **5**, 131 (1983).

[70] W. L. Mengeling, Prenatal infection following maternal exposure to porcine parvovirus on either the seventh or fourteenth day of gestation, *Can. J. Comp. Med.* **43**, 106 (1979).

[71] W. L. Mengeling and R. C. Cutlip, Reproductive disease experimentally induced by exposing pregnant gilts to porcine parvovirus, *Am. J. Vet. Res.* **37**, 1393 (1976).

[72] J. I. Kresse, W. D. Taylor, W. W. Stewart, and K. A. Eernisse, Parvovirus infection in pigs with necrotic and vesicle-like lesions, *Vet. Microbiol.* **10**, 525 (1985).

[73] K. I. Berns and S. Adler, Separation of two types of adeno-associated virus particles containing complementary polynucleotide chains, *J. Virol.* **9**, 394 (1972).

[74] E. Lusby, K. H. Fife, and K. I. Berns, Nucleotide sequence of the inverted terminal repetition in adeno-associated virus DNA, *J. Virol.* **34**, 402 (1980).

[75] M. R. Green and R. G. Roeder, Definition of a novel promoter for the major adenovirus-associated virus mRNA, *Cell* **22**, 231 (1980).

[76] E. W. Lusby and K. I. Berns, Mapping of the 5' termini of two adeno-associated virus 2 RNAs in the left half of the genome, *J. Virol.* **41**, 518 (1982).

[77] R. W. Atchison, The role of herpesviruses in adenovirus-associated virus replication in vitro, *Virology* **42**, 155 (1970).

[78] R. M. Buller, J. E. Janik, E. D. Sebring, and J. A. Rose, Herpes simplex virus types 1 and 2 completely help adenovirus-associated virus replication, *J. Virol.* **40**, 241 (1981).

[79] M. D. Hoggan, N. R. Blacklow, and W. P. Rowe, Studies of small DNA viruses found in various adenovirus preparations: physical, biological, and immunological characteristics, *Proc. Natl. Acad. Sci. U.S.A.* **55**, 1467 (1966).

[80] R. M. Kotin, M. Siniscalco, R. J. Samulski, X. D. Zhu, L. Hunter, C. A. Laughlin, S. McLaughlin, N. Muzyczka, M. Rocchi, and K. I. Berns, Site-specific integration by adeno-associated virus, *Proc. Natl. Acad. Sci. U.S.A.* **87**, 2211 (1990).

[81] R. M. Kotin, J. C. Menninger, D. C. Ward, and K. I. Berns, Mapping and direct visualization of a region-specific viral DNA integration site on chromosome 19q13-qter, *Genomics* **10**, 831 (1991).

[82] R. M. Kotin, R. M. Linden, and K. I. Berns, Characterization of a preferred site on human chromosome 19q for integration of adeno-associated virus DNA by non-homologous recombination, *EMBO J.* **11**, 5071 (1992).

[83] R. J. Samulski, X. Zhu, X. Xiao, J. D. Brook, D. E. Housman, N. Epstein, and L. A. Hunter, Targeted integration of adeno-associated virus (AAV) into human chromosome 19, *EMBO J.* **10**, 3941 (1991).

[84] S. Daya and K. I. Berns, Gene therapy using adeno-associated virus vectors, *Clin. Microbiol. Rev.* **21**, 583 (2008).

[85] F. Mingozzi and K. A. High, Therapeutic in vivo gene transfer for genetic disease using AAV: progress and challenges, *Nat. Rev. Genet.* **12**, 341 (2011).

[86] V. Deiss, J. D. Tratschin, M. Weitz, and G. Siegl, Cloning of the human parvovirus B19 genome and structural analysis of its palindromic termini, *Virology* **175**, 247 (1990).

[87] C. Doerig, P. Beard, and B. Hirt, A transcriptional promoter of the human parvovirus B19 active in vitro and in vivo, *Virology* **157**, 539 (1987).

[88] K. Ozawa, J. Ayub, Y. S. Hao, G. Kurtzman, T. Shimada, and N. Young, Novel transcription map for the B19 (human) pathogenic parvovirus, *J. Virol.* **61**, 2395 (1987).

[89] E. D. Heegaard and K. E. Brown, Human parvovirus B19, *Clin. Microbiol. Rev.* **15**, 485 (2002).

[90] L. KILHAM and L. J. OLIVIER, A latent virus of rats isolated in tissue culture, *Virology* **7**, 428 (1959).

[91] R. C. BATES, C. E. SNYDER, P. T. BANERJEE, and S. MITRA, Autonomous parvovirus LuIII encapsidates equal amounts of plus and minus DNA strands, *J. Virol.* **49**, 319 (1984).

[92] C. R. ASTELL, M. THOMSON, M. MERCHLINSKY, and D. C. WARD, The complete DNA sequence of minute virus of mice, an autonomous parvovirus, *Nucleic Acids Res.* **11**, 999 (1983).

[93] D. PINTEL, D. DADACHANJI, C. R. ASTELL, and D. C. WARD, The genome of minute virus of mice, an autonomous parvovirus, encodes two overlapping transcription units, *Nucleic Acids Res.* **11**, 1019 (1983).

[94] C. HALLAUER, G. SIEGL, and G. KRONAUER, Parvoviruses as contaminants of permanent human cell lines. 3. Biological properties of the isolated viruses, *Arch Gesamte Virusforsch* **38**, 366 (1972).

[95] P. TATTERSALL, The evolution of parvovirus taxonomy, in *Parvoviruses*, edited by J. R. KERR, M. E. BLOOM, S. COTMORE, R. M. LINDEN, and C. R. PARRISH, p. 9, Hodder Arnold, London, UK, 2006.

[96] M. S. JONES, A. KAPOOR, V. V. LUKASHOV, P. SIMMONDS, F. HECHT, and E. DELWART, New DNA viruses identified in patients with acute viral infection syndrome, *J. Virol.* **79**, 8230 (2005).

[97] C. P. SHARP, M. LEBRETON, K. KANTOLA, A. NANA, J. L. E. D. DIFFO, C. F. DJOKO, U. TAMOUFE, J. A. KIYANG, T. G. BABILA, E. M. NGOLE, O. G. PYBUS, E. DELWART, E. DELAPORTE, M. PEETERS, M. SODERLUND-VENERMO, K. HEDMAN, N. D. WOLFE, and P. SIMMONDS, Widespread infection with homologues of human parvoviruses B19, PARV4, and human bocavirus of chimpanzees and gorillas in the wild, *J. Virol.* **84**, 10289 (2010).

[98] S. K. LAU, P. C. WOO, H. TSE, C. T. FU, W. K. AU, X. C. CHEN, H. W. TSOI, T. H. TSANG, J. S. CHAN, D. N. TSANG, K. S. LI, C. W. TSE, T. K. NG, O. T. TSANG, B. J. ZHENG, S. TAM, K. H. CHAN, B. ZHOU, and K. Y. YUEN, Identification of novel porcine and bovine parvoviruses closely related to human parvovirus 4, *J. Gen. Virol.* **89**, 1840 (2008).

[99] C. ADLHOCH, M. KAISER, H. ELLERBROK, and G. PAULI, High prevalence of porcine Hokovirus in German wild boar populations, *Virol. J.* **7**, 171 (2010).

[100] B. Li, J. Ma, S. Xiao, L. Wen, Y. Ni, X. Zhang, L. Fang, and K. He, Genome sequence of a highly prevalent porcine partetravirus in Mainland China, *J. Virol.* **86**, 1899 (2012).

[101] H. Tse, H. W. Tsoi, J. L. Teng, X. C. Chen, H. Liu, B. Zhou, B. J. Zheng, P. C. Woo, S. K. Lau, and K. Y. Yuen, Discovery and genomic characterization of a novel ovine partetravirus and a new genotype of bovine partetravirus, *PLoS ONE* **6**, e25619 (2011).

[102] S. Lou, B. Xu, Q. Huang, N. Zhi, F. Cheng, S. Wong, K. Brown, E. Delwart, Z. Liu, and J. Qiu, Molecular characterization of the newly identified human parvovirus 4 in the family Parvoviridae, *Virology* **422**, 59 (2012).

[103] H. K. Jindal, C. B. Yong, G. M. Wilson, P. Tam, and C. R. Astell, Mutations in the NTP-binding motif of minute virus of mice (MVM) NS-1 protein uncouple ATPase and DNA helicase functions, *J. Biol. Chem.* **269**, 3283 (1994).

[104] S. L. Walker, R. S. Wonderling, and R. A. Owens, Mutational analysis of the adeno-associated virus type 2 Rep68 protein helicase motifs, *J. Virol.* **71**, 6996 (1997).

[105] M. Momoeda, S. Wong, M. Kawase, N. S. Young, and S. Kajigaya, A putative nucleoside triphosphate-binding domain in the nonstructural protein of B19 parvovirus is required for cytotoxicity, *J. Virol.* **68**, 8443 (1994).

[106] R. Simmons, C. Sharp, C. P. McClure, J. Rohrbach, H. Kovari, and et al., Parvovirus 4 infection and clinical outcome in high-risk populations, *J. Infect. Dis.* **205**, 1816 (2012).

[107] X. Yu, J. Zhang, L. Hong, J. Wang, Z. Yuan, X. Zhang, and R. Ghildyal, High prevalence of human parvovirus 4 infection in HBV and HCV infected individuals in shanghai, *PLoS ONE* **7**, e29474 (2012).

[108] A. Manning, S. J. Willey, J. E. Bell, and P. Simmonds, Comparison of tissue distribution, persistence, and molecular epidemiology of parvovirus B19 and novel human parvoviruses PARV4 and human bocavirus, *J. Infect. Dis.* **195**, 1345 (2007).

[109] R. Simmons, C. Sharp, J. Levine, P. Bowness, P. Simmonds, A. Cox, and P. Klenerman, Evolution of CD8+ T cell responses after acute PARV4 infection, *J. Virol.* **87**, 3087 (2013).

[110] C. P. SHARP, A. LAIL, S. DONFIELD, E. D. GOMPERTS, and P. SIMMONDS, Virologic and clinical features of primary infection with human parvovirus 4 in subjects with hemophilia: frequent transmission by virally inactivated clotting factor concentrates, *Transfusion* **52**, 1482 (2012).

[111] M. LAVOIE, C. P. SHARP, J. PEPIN, C. PENNINGTON, Y. FOUPOUAPOUOGNIGNI, O. G. PYBUS, R. NJOUOM, and P. SIMMONDS, Human parvovirus 4 infection, Cameroon, *Emerging Infect. Dis.* **18**, 680 (2012).

[112] M. PANNING, R. KOBBE, S. VOLLBACH, J. F. DREXLER, S. ADJEI, O. ADJEI, C. DROSTEN, J. MAY, and A. M. EIS-HUBINGER, Novel human parvovirus 4 genotype 3 in infants, Ghana, *Emerging Infect. Dis.* **16**, 1143 (2010).

[113] L. J. BALL-GOODRICH, R. D. MOIR, and P. TATTERSALL, Parvoviral target cell specificity: acquisition of fibrotropism by a mutant of the lymphotropic strain of minute virus of mice involves multiple amino acid substitutions within the capsid, *Virology* **184**, 175 (1991).

[114] B. A. SPALHOLZ and P. TATTERSALL, Interaction of minute virus of mice with differentiated cells: strain-dependent target cell specificity is mediated by intracellular factors, *J. Virol.* **46**, 937 (1983).

[115] P. TATTERSALL and J. BRATTON, Reciprocal productive and restrictive virus-cell interactions of immunosuppressive and prototype strains of minute virus of mice, *J. Virol.* **46**, 944 (1983).

[116] J. P. ANTONIETTI, R. SAHLI, P. BEARD, and B. HIRT, Characterization of the cell type-specific determinant in the genome of minute virus of mice, *J. Virol.* **62** (1988).

[117] M. C. COLOMAR, B. HIRT, and P. BEARD, Two segments in the genome of the immunosuppressive minute virus of mice determine the host-cell specificity, control viral DNA replication and affect viral RNA metabolism, *J. Gen. Virol.* **79 (Pt 3)**, 581 (1998).

[118] I. H. MAXWELL, A. L. SPITZER, F. MAXWELL, and D. J. PINTEL, The capsid determinant of fibrotropism for the MVMp strain of minute virus of mice functions via VP2 and not VP1, *J. Virol.* **69**, 5829 (1995).

[119] L. J. BALL-GOODRICH and P. TATTERSALL, Two amino acid substitutions within the capsid are coordinately required for acquisition of fibrotropism by the lymphotropic strain of minute virus of mice, *J. Virol.* **66**, 3415 (1992).

[120] E. M. GARDINER and P. TATTERSALL, Evidence that developmentally regulated control of gene expression by a parvoviral allotropic determinant is particle mediated, *J. Virol.* **62**, 1713 (1988).

[121] E. M. GARDINER and P. TATTERSALL, Mapping of the fibrotropic and lymphotropic host range determinants of the parvovirus minute virus of mice, *J. Virol.* **62**, 2605 (1988).

[122] L. GOVINDASAMY, K. HUEFFER, C. R. PARRISH, and M. AGBANDJE-MCKENNA, Structures of host range-controlling regions of the capsids of canine and feline parvoviruses and mutants, *J. Virol.* **77**, 12211 (2003).

[123] K. HUEFFER, L. GOVINDASAMY, M. AGBANDJE-MCKENNA, and C. R. PARRISH, Combinations of two capsid regions controlling canine host range determine canine transferrin receptor binding by canine and feline parvoviruses, *J. Virol.* **77**, 10099 (2003).

[124] J. VASUDEVACHARYA and R. W. COMPANS, The NS and capsid genes determine the host range of porcine parvovirus, *Virology* **187**, 515 (1992).

[125] M. AGBANDJE-MCKENNA, A. L. LLAMAS-SAIZ, F. WANG, P. TATTERSALL, and M. G. ROSSMANN, Functional implications of the structure of the murine parvovirus, minute virus of mice, *Structure* **6**, 1369 (1998).

[126] P. B. KIMSEY, H. D. ENGERS, B. HIRT, and C. V. JONGENEEL, Pathogenicity of fibroblast- and lymphocyte-specific variants of minute virus of mice, *J. Virol.* **59**, 8 (1986).

[127] D. G. BROWNSTEIN, A. L. SMITH, E. A. JOHNSON, D. J. PINTEL, L. K. NAEGER, and P. TATTERSALL, The pathogenesis of infection with minute virus of mice depends on expression of the small nonstructural protein NS2 and on the genotype of the allotropic determinants VP1 and VP2, *J. Virol.* **66**, 3118 (1992).

[128] D. G. BROWNSTEIN, A. L. SMITH, R. O. JACOBY, E. A. JOHNSON, G. HANSEN, and P. TATTERSALL, Pathogenesis of infection with a virulent allotropic variant of minute virus of mice and regulation by host genotype, *Lab. Invest.* **65**, 357 (1991).

[129] J. C. SEGOVIA, J. A. BUEREN, and J. M. ALMENDRAL, Myeloid depression follows infection of susceptible newborn mice with the parvovirus minute virus of mice (strain i), *J. Virol.* **69**, 3229 (1995).

[130] J. C. Ramirez, A. Fairen, and J. M. Almendral, Parvovirus minute virus of mice strain i multiplication and pathogenesis in the newborn mouse brain are restricted to proliferative areas and to migratory cerebellar young neurons, *J. Virol.* **70**, 8109 (1996).

[131] R. Itah, J. Tal, and C. Davis, Host cell specificity of minute virus of mice in the developing mouse embryo, *J. Virol.* **78**, 9474 (2004).

[132] G. C. Bosma, R. P. Custer, and M. J. Bosma, A severe combined immunodeficiency mutation in the mouse, *Nature* **301**, 527 (1983).

[133] J. C. Segovia, G. Guenechea, J. M. Gallego, J. M. Almendral, and J. A. Bueren, Parvovirus infection suppresses long-term repopulating hematopoietic stem cells, *J. Virol.* **77**, 8495 (2003).

[134] J. C. Segovia, J. M. Gallego, J. A. Bueren, and J. M. Almendral, Severe leukopenia and dysregulated erythropoiesis in SCID mice persistently infected with the parvovirus minute virus of mice, *J. Virol.* **73**, 1774 (1999).

[135] A. Lopez-Bueno, M. P. Rubio, N. Bryant, R. McKenna, M. Agbandje-McKenna, and J. M. Almendral, Host-selected amino acid changes at the sialic acid binding pocket of the parvovirus capsid modulate cell binding affinity and determine virulence, *J. Virol.* **80**, 1563 (2006).

[136] M. P. Rubio, A. Lopez-Bueno, and J. M. Almendral, Virulent variants emerging in mice infected with the apathogenic prototype strain of the parvovirus minute virus of mice exhibit a capsid with low avidity for a primary receptor, *J. Virol.* **79**, 11280 (2005).

[137] A. Lopez-Bueno, J. C. Segovia, J. A. Bueren, M. G. O'Sullivan, F. Wang, P. Tattersall, and J. M. Almendral, Evolution to pathogenicity of the parvovirus minute virus of mice in immunodeficient mice involves genetic heterogeneity at the capsid domain that determines tropism, *J. Virol.* **82**, 1195 (2008).

[138] M. E. Bloom, B. D. Berry, W. Wei, S. Perryman, and J. B. Wolfinbarger, Characterization of chimeric full-length molecular clones of Aleutian mink disease parvovirus (ADV): identification of a determinant governing replication of ADV in cell culture, *J. Virol.* **67**, 5976 (1993).

[139] J. Bergeron, B. Hebert, and P. Tijssen, Genome organization of the Kresse strain of porcine parvovirus: identification of the allotropic determinant and comparison with those of NADL-2 and field isolates, *J. Virol.* **70**, 2508 (1996).

[140] C. R. PARRISH, C. F. AQUADRO, and L. E. CARMICHAEL, Canine host range and a specific epitope map along with variant sequences in the capsid protein gene of canine parvovirus and related feline, mink, and raccoon parvoviruses, *Virology* **166**, 293 (1988).

[141] S. F. CHANG, J. Y. SGRO, and C. R. PARRISH, Multiple amino acids in the capsid structure of canine parvovirus coordinately determine the canine host range and specific antigenic and hemagglutination properties, *J. Virol.* **66**, 6858 (1992).

[142] U. TRUYEN, M. AGBANDJE, and C. R. PARRISH, Characterization of the feline host range and a specific epitope of feline panleukopenia virus, *Virology* **200**, 494 (1994).

[143] M. AGBANDJE-MCKENNA and M. S. CHAPMAN, Correlating structure with function in the viral capsid, in *Parvoviruses*, edited by J. R. KERR, M. E. BLOOM, S. COTMORE, R. M. LINDEN, and C. R. PARRISH, pp. 125–139, Hodder Arnold, London, UK, 2006.

[144] K. HUEFFER and C. R. PARRISH, Parvovirus host range, cell tropism and evolution, *Curr. Opin. Microbiol.* **6**, 392 (2003).

[145] N. PREVISANI, S. FONTANA, B. HIRT, and P. BEARD, Growth of the parvovirus minute virus of mice MVMp3 in EL4 lymphocytes is restricted after cell entry and before viral DNA amplification: cell-specific differences in virus uncoating in vitro, *J. Virol.* **71**, 7769 (1997).

[146] M. HORIUCHI, N. ISHIGURO, H. GOTO, and M. SHINAGAWA, Characterization of the stage(s) in the virus replication cycle at which the host-cell specificity of the feline parvovirus subgroup is regulated in canine cells, *Virology* **189**, 600 (1992).

[147] C. ROS, C. BALTZER, B. MANI, and C. KEMPF, Parvovirus uncoating in vitro reveals a mechanism of DNA release without capsid disassembly and striking differences in encapsidated DNA stability, *Virology* **345**, 137 (2006).

[148] M. AGBANDJE, C. PARRISH, and M. ROSSMANN, The structure of parvoviruses, *Seminars in Virology* **6**, 299 (1995).

[149] M. AGBANDJE, R. MCKENNA, M. G. ROSSMANN, M. L. STRASSHEIM, and C. R. PARRISH, Structure determination of feline panleukopenia virus empty particles, *Proteins* **16**, 155 (1993).

[150] A. A. SIMPSON, B. HEBERT, G. M. SULLIVAN, C. R. PARRISH, Z. ZADORI, P. TIJSSEN, and M. G. ROSSMANN, The structure of porcine parvovirus: comparison with related viruses, *J. Mol. Biol.* **315**, 1189 (2002).

[151] J. TSAO, M. S. CHAPMAN, M. AGBANDJE, W. KELLER, K. SMITH, H. WU, M. LUO, T. J. SMITH, M. G. ROSSMANN, and R. W. COMPANS, The three-dimensional structure of canine parvovirus and its functional implications, *Science* **251**, 1456 (1991).

[152] A. L. LLAMAS-SAIZ, M. AGBANDJE-MCKENNA, W. R. WIKOFF, J. BRATTON, P. TATTERSALL, and M. G. ROSSMANN, Structure determination of minute virus of mice, *Acta Crystallogr. D Biol. Crystallogr.* **53**, 93 (1997).

[153] M. G. ROSSMANN and J. E. JOHNSON, Icosahedral RNA virus structure, *Annu. Rev. Biochem.* **58**, 533 (1989).

[154] H. WU, W. KELLER, and M. G. ROSSMANN, Determination and refinement of the canine parvovirus empty-capsid structure, *Acta Crystallogr. D Biol. Crystallogr.* **49**, 572 (1993).

[155] Q. XIE and M. S. CHAPMAN, Canine parvovirus capsid structure, analyzed at 2.9 A resolution, *J. Mol. Biol.* **264**, 497 (1996).

[156] M. S. CHAPMAN and M. G. ROSSMANN, Structure, sequence, and function correlations among parvoviruses, *Virology* **194**, 491 (1993).

[157] M. S. CHAPMAN and M. G. ROSSMANN, Single-stranded DNA-protein interactions in canine parvovirus, *Structure* **3**, 151 (1995).

[158] J. TSAO, M. S. CHAPMAN, H. WU, M. AGBANDJE, W. KELLER, and M. G. ROSSMANN, Structure determination of monoclinic canine parvovirus, *Acta Crystallogr., B* **48 (Pt 1)**, 75 (1992).

[159] L. A. SALZMAN and W. L. WHITE, Structural proteins of Kilham rat virus, *Biochem. Biophys. Res. Commun.* **41**, 1551 (1970).

[160] J. A. ROSE, J. V. MAIZEL, J. K. INMAN, and A. J. SHATKIN, Structural proteins of adenovirus-associated viruses, *J. Virol.* **8**, 766 (1971).

[161] F. B. JOHNSON, H. L. OZER, and M. D. HOGGAN, Structural proteins of adenovirus-associated virus type 3, *J. Virol.* **8**, 860 (1971).

[162] J. W. LITTLEFIELD, THREE DEGREES OF GUANYLIC ACID–INOSINIC ACID PYROPHOSPHORYLASE DEFICIENCY IN MOUSE FIBROBLASTS, *Nature* **203**, 1142 (1964).

[163] H. M. SHEIN and J. F. ENDERS, Multiplication and cytopathogenicity of Simian vacuolating virus 40 in cultures of human tissues, *Proc. Soc. Exp. Biol. Med.* **109**, 495 (1962).

[164] E. Harlow, L. V. Crawford, D. C. Pim, and N. M. Williamson, Monoclonal antibodies specific for simian virus 40 tumor antigens, *J. Virol.* **39**, 861 (1981).